INFORMATION TO USERS

This manuscript has been reproduced from the microfilm master. UMI films the text directly from the original or copy submitted. Thus, some thesis and dissertation copies are in typewriter face, while others may be from any type of computer printer.

The quality of this reproduction is dependent upon the quality of the copy submitted. Broken or indistinct print, colored or poor quality illustrations and photographs, print bleedthrough, substandard margins, and improper alignment can adversely affect reproduction.

In the unlikely event that the author did not send UMI a complete manuscript and there are missing pages, these will be noted. Also, if unauthorized copyright material had to be removed, a note will indicate the deletion.

Oversize materials (e.g., maps, drawings, charts) are reproduced by sectioning the original, beginning at the upper left-hand corner and continuing from left to right in equal sections with small overlaps.

Photographs included in the original manuscript have been reproduced xerographically in this copy. Higher quality 6" x 9" black and white photographic prints are available for any photographs or illustrations appearing in this copy for an additional charge. Contact UMI directly to order.

ProQuest Information and Learning
300 North Zeeb Road, Ann Arbor, MI 48106-1346 USA
800-521-0600

UMI®

Second-harmonic generation as a probe of chemically modified Si(111) surfaces and the initial oxidation of hydrogen terminated Si(111)

Sarah Anderson

A Thesis

in

The Department

of

Chemistry and Biochemistry

Presented in Partial Fulfillment of the Requirements
For the Degree of Master of Science at
Concordia University
Montreal, Quebec, Canada

August 2000

© Sarah Anderson, 2000

National Library of Canada

Bibliothèque nationale du Canada

Acquisitions and Bibliographic Services

Acquisitions et services bibliographiques

395 Wellington Street
Ottawa ON K1A 0N4
Canada

395, rue Wellington
Ottawa ON K1A 0N4
Canada

Your file Votre référence

Our file Notre référence

The author has granted a non-exclusive licence allowing the National Library of Canada to reproduce, loan, distribute or sell copies of this thesis in microform, paper or electronic formats.

L'auteur a accordé une licence non exclusive permettant à la Bibliothèque nationale du Canada de reproduire, prêter, distribuer ou vendre des copies de cette thèse sous la forme de microfiche/film, de reproduction sur papier ou sur format électronique.

The author retains ownership of the copyright in this thesis. Neither the thesis nor substantial extracts from it may be printed or otherwise reproduced without the author's permission.

L'auteur conserve la propriété du droit d'auteur qui protège cette thèse. Ni la thèse ni des extraits substantiels de celle-ci ne doivent être imprimés ou autrement reproduits sans son autorisation.

0-612-59270-7

Canada

ABSTRACT

Second-harmonic generation as a probe of chemically modified Si(111) surfaces and the initial oxidation of hydrogen terminated Si(111)

Sarah Anderson

Optical second-harmonic generation (SHG) is used to probe Si(111) surfaces with covalently attached monolayers. The surfaces are prepared using wet chemical modification to form -H, -$C_{10}H_{21}$ (decyl) and -O-$C_{10}H_{21}$ (decyloxy) monolayers. The SHG efficiency for these surfaces as well as a Si(111) surface with a native oxide film is reported. The signal's intensity and modulation through a 360° rotation, or rotational anisotropy, can be correlated with the substrate's chemical modification. The potential for SHG to be used as a probe for monitoring the initial oxidation of Si(111)-H *in situ* is investigated. The mechanism by which this reaction occurs over time is not well understood. Three environments have been studied: N_2 purge to inhibit oxidation, oxidation in ambient air, and photo-oxidation in ambient air using UV irradiation. Possible processes by which water and molecular oxygen initiate the surface oxidation are identified.

Acknowledgements

After completing my research and weaving my results into an original story over the course of the past two years, I have many people to acknowledge. First and foremost, I could not have done it without Dr. Steven Mitchell, my supervisor at the National Research Council in Ottawa. His knowledge of nonlinear optics and surface chemistry incited me to learn as much as possible about these fascinating fields. He was always willing to answer my questions, and, more importantly, often showed me how I could answer them myself.

I could not have pursued any of this without Dr. John Capobianco, my supervisor at Concordia University either. He recognized the possibilities and benefits of research at a national laboratory and facilitated the means to follow this path. Furthermore, I would like to thank Dr. Peter Bird and Dr. Marcus Lawrence for taking the time to be a part of my thesis committee.

As I embarked on this journey in September 1998, I found myself amidst an excellent team of scientists in the Molecular Interfaces program at NRC's Steacie Institute for Molecular Sciences. Dr. Danial Wayner heads this dynamic group and I am proud to call them my colleagues. I would like to thank Dr. Rabah Boukherroub in particular for all his meticulous organic surface modifications. As well, the Femtosecond Science program deserves recognition for its topnotch laser facility, the source for most of my analytical work. At Concordia, I shared an office with other students under the tutelage of Dr.

Capobianco. I would like to thank them all for their support and friendship. As well, I cannot dismiss the impact that funding from Fonds FCAR, NSERC and NRC has made on my experience as a graduate student.

Finally, I must extend the warmest expression of gratitude to my family for their continued love and encouragement as I achieved each small step towards my goal and a special mention to those who have made a significant impact on my life by believing in me. It's been quite extraordinary.

List of figures ix

1. Introduction

1.1. Nonlinear optics 1

1.1.1. Second-harmonic generation 1

1.1.2. History of surface nonlinear optics 2

1.2 Semiconductors 3

1.3. Si(111) surface 5

1.4. Hydrogen terminated Si(111) surfaces 8

1.5. Organic monolayers on Si(111) 11

1.6. Oxidation of hydrogen terminated silicon surfaces 13

1.7. Motivation to study Si(111)-H and other modified surfaces 21

References 23

2. Theory

2.1. Distinction between linear and nonlinear optics 26

2.2. Optical probes 29

2.3. Harmonic generation at surfaces 33

2.3.1. SHG from a centrosymmetric cubic crystal 33

2.3.2. Rotational anisotropy equations 34

References 38

3. Experimental

3.1. Second-harmonic generation 40

3.1.1. Pellin-Broca prism 41

3.2. Experimental conditions 45

3.2.1. Third-harmonic generation 45

3.2.2. Nitrogen purge 45

3.2.3. Ultraviolet irradiation 45

3.3. Preparation of samples 46

References 48

4. Results and Discussion

4.1. Influence of a center of inversion upon harmonic generation 49

4.2. Comparison of chemically modified Si(111) surfaces 53

4.3. Stability of organic monolayers on Si(111) 59

4.4. Oxidation of Si(111)-H 63

4.4.1. Hydrocarbon surface contamination of Si(111)-H 63

4.4.2. Nitrogen purge 66

4.4.3. Exposure to ambient air in the dark 68

4.5. Photo-oxidation of Si(111)-H 75

4.5.1. 350-nm broadband irradiation in ambient air 75

4.5.2. 254-nm irradiation in ambient air 77

4.5.3. Continuous monitoring of signal during 254-nm irradiation 78

4.5.4. Incremental monitoring of signal during 254-nm irradiation 82

4.5.5. Variation of UV irradiance for continuous monitoring 87

4.6. Chemical mechanism for Si(111)-H oxidation 89

References 92

5. Conclusions 94

References 97

6. Future work 98

References 101

List of figures

1. Introduction

Figure 1.3.1 Cubic and centrosymmetric unit cell of silicon, truncation through atoms with asterisks reveals (111) face 6

Figure 1.3.2a Si(111) atomic structure of topmost bilayer with surface atoms(solid) and back-bonded atoms (open circles) 7

Figure 1.3.2b Perspective view of two bilayers of ideally terminated Si(111)-H with the hydrogen atoms shown as open circles 7

Figure 1.3.3a Contact mode atomic force microscope image of Si(111)-H 9

Figure 1.3.3b Contact mode atomic force microscope image of Si(111)-$C_{10}H_{21}$ 9

Figure 1.4.1 Schematic representation of the mechanism of hydrogen passivation 10

Figure 1.6.1 Oxygen insertion into the structure of a Si(111)-H bilayer 18

2. Theory

Figure 2.1.1 Analysis of a nonlinear polarization wave 28

Figure 2.2.1 Polarization of incident and reflected fundamental and second-harmonic beams and orientation of the Si(111) wafer with respect to the azimuthal rotation angle, ϕ 32

Figure 2.3.1 Contributions to the second-harmonic signal for Si(111), refer to equation 2.3.6 37

3. Experimental

Figure 3.1.1 SHG signal intensity with and without a 46% neutral density filter to attenuate the maximum pulse energy of ~3.0μJ 42

Figure 3.1.2 Pellin-Broca prism 43

4. Results and Discussion

Figure 4.1.1 Comparison of second-harmonic signal 50

Figure 4.1.2 Comparison of third-harmonic signal 51

Figure 4.2.1 Comparison of chemically modified Si(111) surfaces at λ = 830 nm 54

Figure 4.2.2 Comparison of chemically modified Si(111) surfaces at λ = 830 nm 55

Figure 4.2.3 Comparison of chemically modified Si(111) surfaces at λ = 830 nm 56

Figure 4.2.4 Comparison of decyloxy modified surface prepared by reaction with decanal (A) and decanol (B) 58

Figure 4.3.1 Comparison of SHG signal of decyl modified Si(111) surface over 21 days 60

Figure 4.3.2 Comparison of SHG signal of decyloxy modified Si(111) surface, prepared by reaction with decanal, over 7 days 62

Figure 4.3.3 Comparison of SHG signal of decyloxy modified Si(111) surface, prepared by reaction with decanol, over 1 day 64

Figure 4.4.1 Monitoring of Si(111)-H in nitrogen purge 67

Figure 4.4.2	Evolution of Si(111)-H surface oxidation over time in ambient air in the dark	69
Figure 4.4.3	Evolution of Si(111)-H surface oxidation over time in ambient air in the dark	70
Figure 4.4.4	Evolution over time of SHG parameters for Si(111)-H oxidation in ambient air in the dark	71
Figure 4.5.1	Comparison of the evolution of Si(111)-H surface oxidation over time, with and without broadband 350-nm irradiation, in ambient air	76
Figure 4.5.2a	Si(111)-H surface monitored 19 days after fresh preparation	80
Figure 4.5.2b	Si(111)-H Surface monitored 30 minutes of fresh preparation	80
Figure 4.5.3	Evolution of Si(111)-H surface oxidation over time as a function of UV irradiation in ambient air. Dashed line in top plot is native oxide SHG signal	83
Figure 4.5.4	Evolution of Si(111)-H surface oxidation over time as a function of UV irradiation in ambient air. Dashed line in top plot is native oxide SHG signal	85
Figure 4.5.5	Evolution over time of SHG parameters for Si(111)-H oxidation as a function of UV exposure	86
Figure 4.5.6	Continuous monitoring of the anisotropic signal for Si(111)-H as a function of UV irradiance	88
Figure 4.5.7	Water attack of Si-Si back bonds of a Si(111)-H surface	91
Figure 4.5.8	Water attack of the Si-H bond of a Si(111)-H surface	91

1. Introduction

1.1. Nonlinear optics

1.1.1. Second-harmonic generation

Optical second-harmonic generation (SHG) is the nonlinear conversion of two photons of frequency ω to one photon of frequency 2ω. When an optical wave at frequency ω impinges on a medium, the wave induces a dipole oscillation of each molecule in the medium. At high field strengths, a molecule behaves like an anharmonic oscillator and overtone oscillations are excited. Oscillating dipoles emit electromagnetic radiation, so output at the overtone frequencies 2ω, 3ω and so on as well as the fundamental frequency ω, is expected [1]. For a driven anharmonic oscillator, the induced dipole component, $p(2\omega)$ is proportional to the quantity $E(\omega)E(\omega)$, the 'self product' of the incoming field of strength E, at frequency ω. The induced second-harmonic dipole per unit volume, or polarization, $P^{(2)}(2\omega)$ can be written as

$$P^{(2)}(2\omega) = \chi^{(2)} E(\omega)E(\omega) \qquad 1.1.1$$

where $\chi^{(2)}$ is the macroscopic nonlinear susceptibility tensor and is a characteristic coefficient of the medium [1]. If the medium possesses inversion symmetry, the incoming fields E and –E must induce dipoles of P and –P respectively. This is inconsistent with Equation 1.1.1 unless $\chi^{(2)}$ equals zero, indicating that SHG is forbidden [1].

Optical SHG requires a noncentrosymmetric[1] medium, and this type of crystal is employed for frequency doubling in a wide variety of laser systems. Perhaps the most familiar instance of this phenomenon is the conversion of 1064 nm near infrared light to 532 nm green light in a Nd^{3+}:YAG laser. Alternately, SHG can be obtained by the break in symmetry that occurs at the interface between two centrosymmetric media. Nonlinear effects are therefore allowed and, since it is only the first few monolayers on either side of the interface which participate in the lifting of inversion symmetry, the SHG process is a highly surface-selective optical probe [2].

1.1.2. History of surface nonlinear optics

With Maiman's announcement of the first operative ruby laser in 1960, finally a light source capable of nonlinear optical effects existed. Previously, such interactions were not observable due to the small electric fields produced by ordinary light sources. Bright carbon arc lamps were not feasible, as the broad emission spectra made nonlinear effects difficult to find [3]. A great deal of energy needs to be concentrated into a narrow band of wavelengths to allow electromagnetic waves to interact with each other in an orderly way.

The advent of coherent and monochromatic laser light led Franken and co-workers [4] to investigate nonlinear effects in 1961. His group focused a ruby laser beam of 694.3 nm onto a quartz crystal. One part in 10^8 was converted to a highly directional beam of exactly 347.15 nm; thus, there was no mistaking the second harmonic, as this wavelength

[1] a material lacking inversion symmetry

was precisely half that of the incident light. By means of nonlinear processes, it was evident that a whole new range of wavelengths in the infrared, visible and ultraviolet regions of the electromagnetic spectrum would become available [3]. In 1965, Brown et al. [5] published a journal article entitled "Nonlinear optical reflection from a metallic boundary", marking the first instance of SHG observed from a centrosymmetric isotropic material. Franken's experiment produced a bulk response because quartz is noncentrosymmetric. Brown's result, achieved using silver films evaporated onto a prism, illustrated the surface sensitivity of SHG attainable with centrosymmetric media. Since then, researchers have expanded the breadth of knowledge in the field of surface nonlinear optics with materials such as silicon, which has an anisotropic[2] response in the nonlinear regime. Bloembergen [6] designated the sixties as the period of 'classical antiquity' for SHG at interfaces, the seventies as the Middle Ages, with the Renaissance starting in 1980. This renewed interest came rather by accident as surface-enhanced Raman scattering attracted attention in the physics community and questions were posed about exploring the surface sensitivity of SHG [7]. Latterly, the scope of SHG measurements has ranged from probing liquid crystal surfaces and polymer interfaces to thin films of C_{60} and chiral molecules [6].

1.2 Semiconductors

A semiconductor is a crystalline or amorphous solid whose electrical conductivity is typically intermediate between that of a metal and an insulator. The energy level structure

[2] a medium with orientation-dependent macroscopic optical properties

of a semiconductor is comprised of groups of closely spaced levels that form bands [8]. At 0 K, these bands are either completely occupied by electrons or completely empty. The highest filled band is the valence band and the empty band above it is called the conduction band. These two bands are separated by an energy gap on the order of 1 to 3 eV [9]. For silicon, the energy gap is ~ 1 eV. Due to this narrow gap in a semiconductor, thermal population of the conduction band is facile. This is most probable at high temperatures, so conductivity increases rapidly with temperature; while, the conductivity of metals decreases with temperature.

There are both positive and negative charge carriers in a semiconductor. When an electron moves from the valence band to the conduction band, it leaves behind a vacant crystal site or 'hole' in the otherwise filled valence band. This electron deficient hole appears as h^+, a charge carrier. A nearby valence electron can transfer into the hole, allowing the hole to migrate through the material. In a pure or *intrinsic* semiconductor, there are equal numbers of conduction electrons and holes, otherwise known as 'electron-hole pairs'. In the presence of an electric field, holes move in the direction of the field and conduction electrons move in the opposite direction.

When a semiconductor is doped, it is considered *extrinsic*. It can become either n- or p-type depending on the atom that is used as a dopant. If a five valence electron atom, like phosphorus, is added to silicon, four electrons participate in covalent bonds and one lies just below the conduction band and donates to the conduction band. This is n-type conductivity where the charge carriers are electrons. In p-type semiconductors, a three

valence electron atom, such as boron, is added. Since this atom has one fewer electron than silicon, it captures an electron from the valence band. This leaves behind a hole, which acts as an acceptor state for valence band electrons.

The first systematic application of SHG to the study of adsorption at semiconductor surfaces was performed by Chen et al., who monitored the adsorption of alkali metals onto germanium in ultra-high vacuum (UHV) [2]. Since those initial experiments, the vast majority of SHG measurements at semiconductor surfaces have been performed on silicon surfaces. Specifically, the chemisorption of gold, hydrogen and oxide layers have been studied extensively. Organic monolayers have received less scrutiny and attention.

1.3. Si(111) surface

Figure 1.3.1 illustrates the unit cell for silicon, which is cubic and centrosymmetric. Truncation at the three atoms marked with asterisks would reveal the (111) face. At the surface of a medium, inversion symmetry is clearly broken, leaving the Si-Si back bonds of Figure 1.3.2a in a noncentrosymmetric environment. This condition makes a second-order response allowed in the electric-dipole approximation, so the SHG response is mainly derived from the surface. However, higher-order effects such as quadrupole interaction can generate bulk contributions to the SHG signal [10].

The atomic structure of the Si(111) face is shown in Figure 1.3.2a. If only the very topmost atoms (solid circles) are included, the surface belongs to the C_{6v} point group.

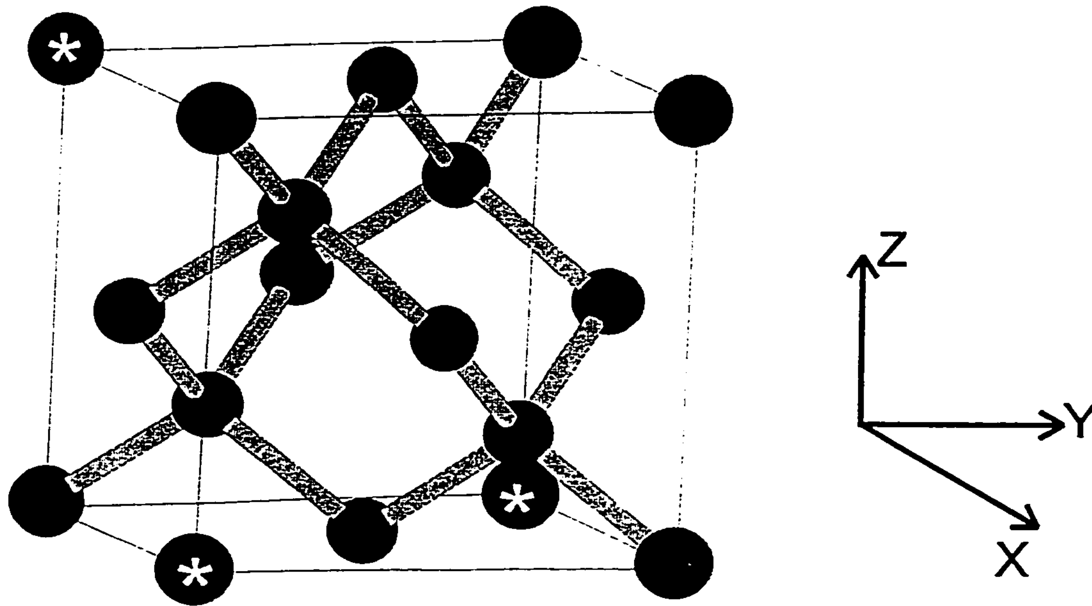

Figure 1.3.1 Cubic and centrosymmetric unit cell of silicon, truncation through atoms with asterisks reveals (111) face

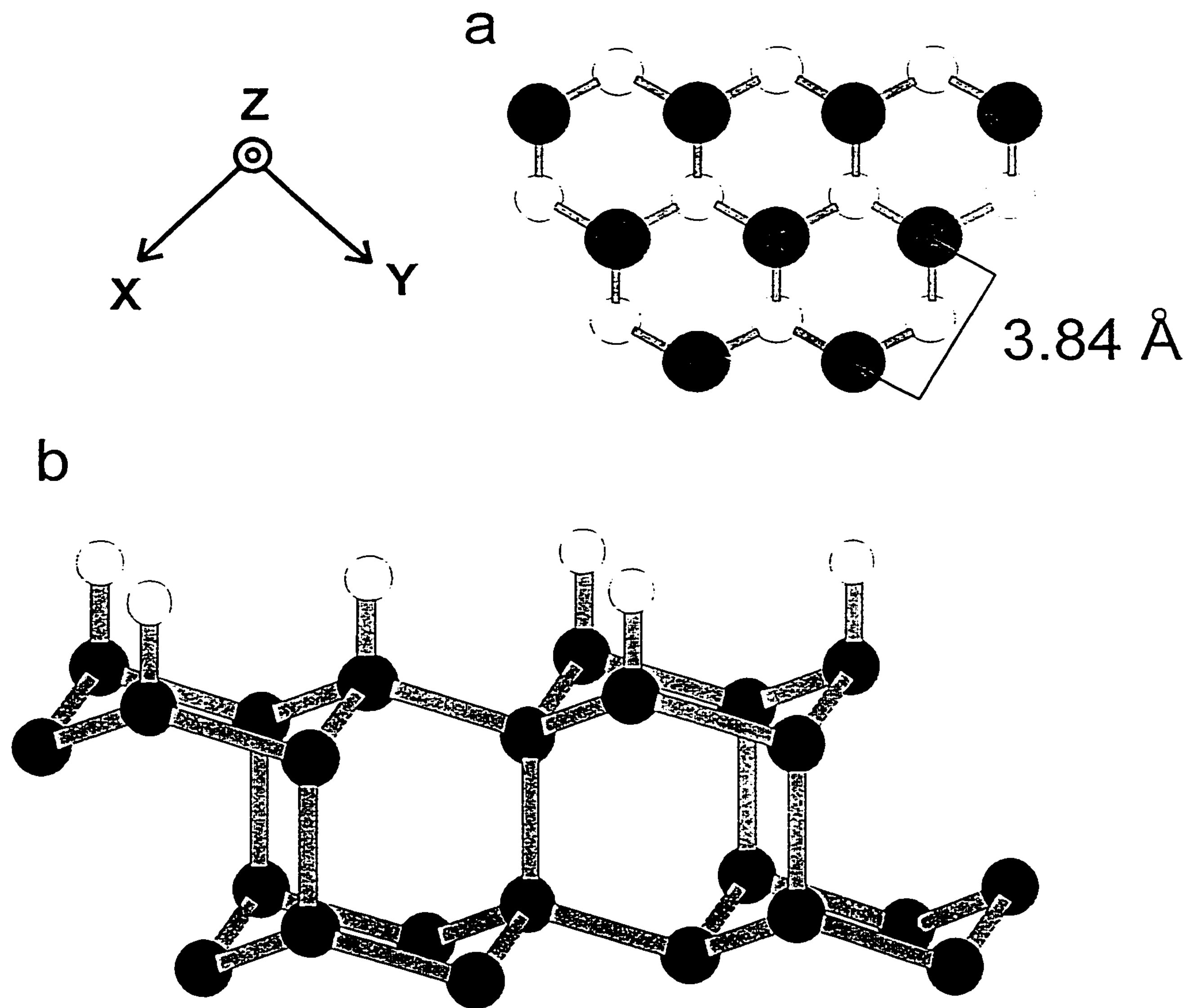

Figure 1.3.2a Si(111) atomic structure of topmost bilayer with surface atoms (solid) and back-bonded atoms (open circles)

Figure 1.3.2b Perspective view of two bilayers of ideally terminated Si(111)-H with the hydrogen atoms shown as open circles

However, taking into consideration an additional surface layer (open circles), the surface possesses C_{3v} symmetry. This is based on the assumption that the surface has a simple unreconstructed structure and thus, for a particular face, has the same symmetry as the bulk [11]. Each surface silicon atom has a trigonal arrangement of back bonds connecting it to the second layer of atoms in the bilayer and a fourth bond which is the dangling bond normal to the surface. This bond can be terminated with species such as hydrogen or alkyl chains.

Figure 1.3.2b represents a perspective view of two bilayers of a Si(111)-H surface with the hydrogen atoms shown as open circles. Figure 1.3.3.a and b are contact mode atomic force microscope (AFM) images of a Si(111)-H and Si(111)-$C_{10}H_{21}$ surface [12], respectively. The width difference for the steps can be attributed to slight differences in the wafer miscut. The wide terraces, with step height of approximately 3Å, indicate that the surfaces are ordered and atomically flat.

1.4 Hydrogen terminated Si(111) surfaces

Etching silicon surfaces with HF acid is a standard method in semiconductor processing to remove the native oxide layer and protect the surface from chemical attack. It has been determined that the concentration of HF affects the morphology of hydrogen terminated surfaces. With dilute HF etchant, the Si(111) surface is atomically rough with mono, di and trihydride species present, observable by Fourier transform infrared (FTIR) spectroscopy. In contrast, the spectrum for the Si(111) surface, prepared in HF solution

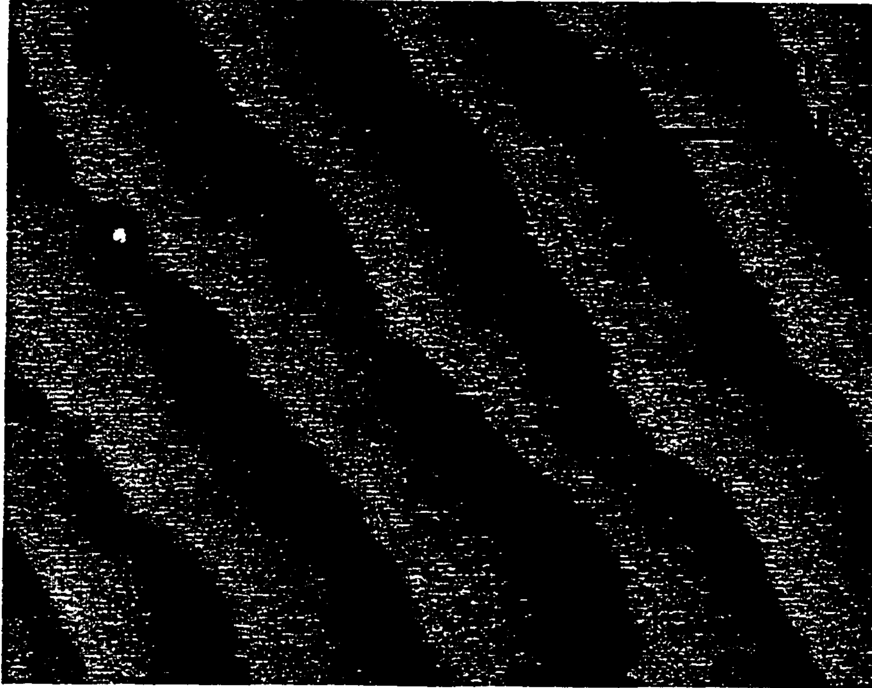

Figure 1.3.3a Contact mode atomic force microscope image of Si(111)-H

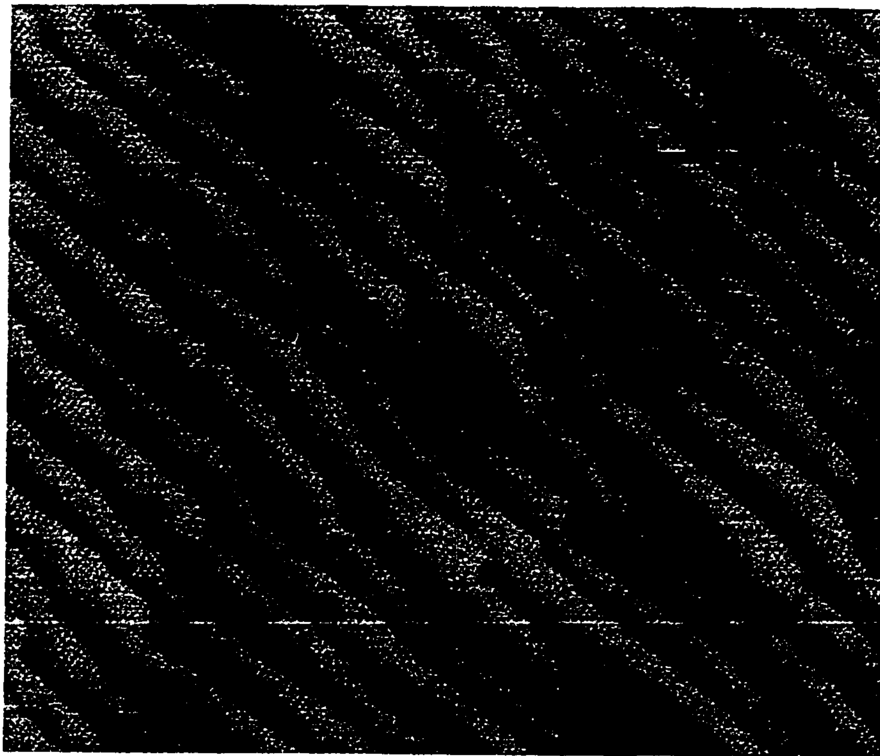

Figure 1.3.3b Contact mode atomic force microscope image of Si(111)-$C_{10}H_{21}$

that is buffered by ammonium fluoride (NH_4F) to pH ~ 9-10, is dominated by a narrow vibrational line at 2083.7 cm^{-1} [13]. The presence of this single mode makes its assignment as the monohydride of an atomically flat hydrogen terminated Si(111) surface indisputable and its sharpness confirms that the Si-H bond is oriented normal to the (111) plane. Since this first preparation of an ideally terminated surface [13], 40% aqueous NH_4F etchant is commonly used.

To understand why hydrogen termination is favored, it is important to interpret the factors inhibiting fluorine termination. Initially, it was suggested that fluorine passivation accounted for the chemical stability of silicon etched in HF [14]. This seemed to be supported by the large difference in bond strengths for Si-F (6.0 eV) versus Si-H (3.5 eV). However, several experimental techniques have now established that H-termination is responsible for the surface passivation. Ubara et al. [15] found that F-terminated silicon complexes are unstable in HF due to the strong polarization of the Si-Si back bonds. This facilitates the attack by HF molecules and results in reactions wherein silicon fluorides are released into solution leaving behind hydrogen atoms bonded to the surface.

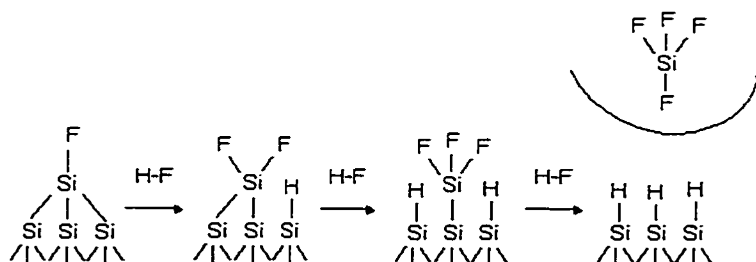

Figure 1.4.1 Schematic representation of the mechanism of hydrogen passivation

Figure 1.4.1, supported by quantum chemical calculations of the activation barriers, illustrates the mechanism of hydrogen passivation [14]. In addition, the reason that HF does not attack the Si-H bonds is elucidated. The activation barrier for this reaction is significantly higher than that for the Si-Si bond cleavage. Overall, reaction kinetics, rather than thermodynamics alone largely determine the hydrogen termination of a silicon surface.

1.5 Organic monolayers on Si(111)

Self-assembled monolayers (SAMs) are ordered molecular assemblies formed by the adsorption of an active surfactant on a solid surface [16]. In contrast to other ultra-thin films, SAMs are highly ordered and oriented, so a variety of surfaces with specific interactions can be produced in a controlled manner. SAMs can have biomimetic properties, useful in biosensor applications and, with high density and stability, they offer potential as protective films against corrosion. Typically, SAMs have been obtained by adsorbing alkanethiols on metal surfaces (gold, silver) or by reacting alkyltrichlorosilanes with hydroxylated surfaces such as SiO_2 or Al_2O_3. There has been much less investigation into achieving direct bonding between an organic monolayer and a semiconductor material [17].

Silicon has a crucial importance in modern technology. Stable, densely packed films in direct contact with this semiconductor surface present new opportunities. The covalent attachment of organic monolayers provides a route to passivation and a method to

integrate chemical and biochemical function into solid-state devices [12]. In synthetic organic chemistry, a variety of chemical reactions can be employed to achieve the same product. Consequently, organic modification of a surface has the same flexibility. The two principal features, which affect the interfacial properties of the material, are film thickness and its chemical composition. The inherent advantage of this method of functionalizing the silicon surface, as compared to the traditional Langmuir-Blodgett organic thin film preparation, is the absence of an oxide layer at the interface which can influence device characteristics [18].

In 1990, the publication of a reproducible preparation of hydrogen terminated silicon surfaces by etching Si(111) single crystals with 40% aqueous NH_4F [13] provided a starting point for new synthetic routes to the formation of organic monolayers on silicon. Three years later, Linford and Chidsey [19] made the first report of densely packed long alkyl chains covalently linked to a silicon surface. This organic modification was achieved by the pyrolysis of neat diacyl peroxides in the presence of Si(111)-H. The nearest neighbor distance between silicon atoms on the (111) surface is 3.84Å; thus, all surface hydrogen atoms cannot be replaced by an alkyl chain (diameter, 4.6Å). Several surface characterization methods confirmed that the alkyl chains were as densely packed as those formed from alkanethiols on gold. Subsequently, these researchers [20] showed that a mixture of an olefin and a diacyl peroxide yielded monolayers with greater stability due to the more uniform coverage obtained, with fewer alkyl chains bound through a hydrolyzable acyloxy linkage to the silicon surface. This improvement occurred because

the majority of the alkyl chains on the surface were olefin-derived and the diacyl peroxide served mainly as a free radical initiator.

Since this seminal work, Wayner and co-workers [12] have formed Si-C monolayers from reactions with Si(111)-H by two methods: thermal reaction of decylmagnesium bromide and Lewis acid catalyzed hydrosilylation of decene. They compared their modified surfaces with one prepared by a photochemical method previously published by Chidsey [21]. All three techniques produce surfaces with similar characteristics, including chemical stability over several weeks. Subsequently, Wayner and co-workers [22] have reported two thermal routes to produce an alkoxy (Si-OR) linkage: direct reaction of alcohols and aldehydes with Si(111)-H. The same modified surface is obtained in both cases, verified by FTIR and X-ray photoelectron spectroscopy (XPS).

1.6 Oxidation of hydrogen terminated silicon surfaces

In the semiconductor industry, control of the surface reactivity of the silicon substrate is very important. Native oxide films on the silicon surface considerably affect the quality of thin films prepared by either chemical vapor deposition (CVD) or molecular beam epitaxy (MBE) [23]. Precision in the thickness and electrical properties of gate oxide films is required. Consequently, as the pattern dimensions of integrated circuits get smaller and smaller, the growth of native oxide films on silicon has received an increasing amount of attention [24]. A hydrogen terminated silicon surface is relatively inert; however, oxidants in air generate a native oxide film after extended exposure [25].

For the technologically more important Si(100) surface, oxygen and water in air seem to attack Si-Si back bonds preferentially rather than the surface Si-H bonds for the initial stages of oxidation. The Si-H bonds oxidize to form Si-OH bonds only once the back bond oxidation is complete [23]. A similar mechanism has been proposed for porous silicon and the tendency for this to occur was attributed to the weaker binding energy of Si-Si (1.83 eV) bonds in comparison to Si-H (3.5 eV) bonds [26]. Morita et al. [24] suggest that the initial stage of native oxide growth on Si(100) arises at the Si-Si back bonds by the following model: the insertion of oxygen species into Si-Si bonds produces Si-O-Si bonds. The Si-H bonds remain intact and maintain the hydrophobic nature of the surface. The co-existence of water and oxygen is necessary to initiate this oxidation. All the silicon atoms in the topmost layer are oxidized to form an amorphous phase before the underlying layer of Si-Si bonds is subject to oxidation. This layer-by-layer oxide growth was rationalized from the successive step function-like increase in native oxide thickness observed over time, when the wafer was exposed to ambient air. A combination of ellipsometry and XPS was used to determine the thickness of these very thin films.

In addition, the influence of the ambient humidity was studied by placing the Si(100)-H surface in a dry nitrogen environment for one week. The growth of native oxide was limited to 1.9Å thickness, while the same length of exposure to clean room air (relative humidity 42%) produced a 6.7Å film. The oxide thickness formed at room temperature after 10 hours in air is estimated to be extremely negligible (as low as 10^{-13} Å) by extrapolation of thermal oxidation rates at temperatures between 800 and 1050°C [24]. This conjecture that oxide is not grown on a hydrogen terminated silicon surface at room

temperature suggests that the oxidation mechanism in air is completely different than that for thermal oxidation. The high temperatures in the latter process allow passivation of the surface with a thick oxide film. Oxidation in air obtains a very thin film because, upon forming, the oxide layer becomes a barrier to deeper penetration.

In spite of research efforts such as the above, the initial stages of the oxidation process are not well understood on a microscopic scale. A well-defined silicon surface with an ordered structure and a single dangling bond per surface atom simplifies such a task. For this reason, Si(111) has become the favored surface to employ in model studies to investigate oxidative reactions of hydrogen terminated silicon.

Many different techniques have been used to monitor the progress of Si(111)-H oxidation. Scanning tunneling microscopy (STM) is excellent for imaging the surface morphology. It can elucidate the extent and quality of the surface reaction. STM images [27] have probed the structural details of Si(111)-H oxidizing over time. Homogeneous nucleation of randomly distributed oxide clusters predominated in the oxidative attack of the surface. After 7 hours of exposure to moist air, the density of the oxide nuclei on the surface was negligible. Further measurement indicated a slow increase in the number of oxide nuclei, until, after 33 days of exposure, the surface appeared smoother. The authors attribute this change to nearly complete oxidation of the topmost bilayer, because the individual oxide nuclei could no longer be identified and the oxidation was confined almost exclusively to the topmost bilayer. The results suggest a nucleation and growth

scenario where vertical growth of the oxide nuclei is suppressed and lateral oxidation is very slow.

Angermann et al. [28] performed spectroscopic ellipsometry (SE) measurements on Si(111)-H to monitor the surface oxidation. The relative number of Si-H oscillators (N_{rel}), proportional to the number of Si-H bonds at the surface, decreased as a function of storage time in air. The effective thickness of the oxide film increased simultaneously with this reduction in Si-H bonds. A homogeneous SiO_2 layer was assumed and the growth appeared to follow an exponential law, after an initial stage of gradual increase, which ended approximately when N_{rel} equaled zero. During the first 24 hours, according to the SE data, the hydrogen coverage was reduced to less than 50%. After 48 hours of exposure in air, the effective oxide thickness exceeded one monolayer. At this time, oxygen back-bonded defects appeared, determined by surface photovoltage (SPV) measurements, and indicated that hydrogen termination was lost. Further growth on the surface populated the defects correlated to Si^{+2} atoms (SiO_2≡Si-) and showed a decrease in the defects correlated to Si^{+1} atoms (Si_2O≡Si-). These changes were apparent by monitoring the evolution of surface states using SPV.

Photoelectron spectroscopy provides an elemental profile of the surface and chemical shifts indicate oxidation states of the silicon atoms, allowing a determination of the bonding configurations. FTIR spectroscopy has been widely used due to the broad range of structural and mechanistic information it provides. Miura et al. [29] showed, by these two methods, how the oxidation of surface silicon atoms was correlated with native oxide

growth on Si(111) and Si(100) surfaces. Their main finding was a direct link between the decrease in the Si-H infrared peak and the steep increase of native oxide thickness, measured from Si 2*p* core level photoelectron spectra. This information led to the proposal of a two-step process for the oxidation. From results of studies performed under low relative humidity conditions, it was argued that water is responsible for the initial attack of surface silicon atoms to produce hydrogen-associated intermediate oxidation species. The second step involves layer-by-layer growth of native oxide. It was observed that the oxide thickness saturated after long exposure to air, measuring approximately 6Å. Because this second step occurred with a rate independent of humidity, oxygen was considered to contribute primarily to native oxide formation.

Figure 1.6.1 illustrates the two possible positions for atomic oxygen insertion into the structure of a Si(111)-H bilayer: intra- and interbilayer. Sieger et al. [30] have shown that the SiO_2/Si(111) interface is chemically abrupt, suggesting that the top bilayer must be fully oxidized before oxygen proceeds to fill interbilayer bonds. This is supported by Miura's [29] two-step model of Si(111)-H oxidation, which suggests that the top bilayer oxidation occurs, followed by a rapid increase of the oxide thickness. The latter step is an indication of interbilayer oxygen insertion. Calculations [29] showed that the independent and simultaneous incidence of surface silicon atom oxidation and native oxide growth does not reproduce experimental results, further bolstering the notion of a layer-by-layer process.

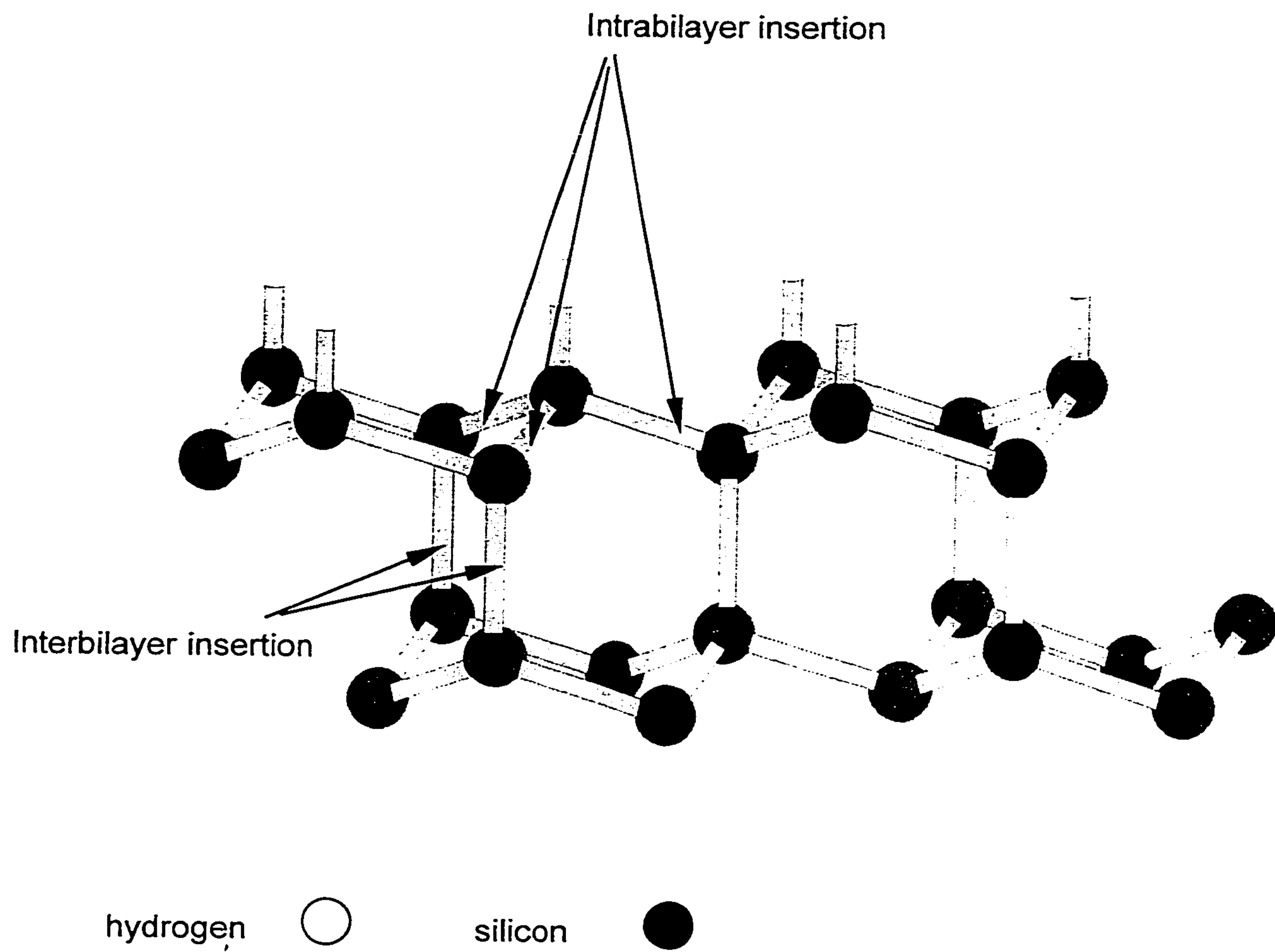

Figure 1.6.1 Oxygen insertion into the structure of a Si(111)-H bilayer

Niwano et al. [25] have undertaken extensive attenuated total reflectance infrared (ATR-IR) spectroscopy studies to determine which oxidant, molecular oxygen or water, is primarily responsible for the oxidation of the topmost layer of hydrogen terminated silicon surfaces. In addition, the time scale for oxidation has been investigated. Infrared spectroscopy is a useful technique because the Si-H vibration frequency has been determined for a silicon atom with different numbers of oxygen and hydrogen atoms bonded to it. For a NH_4F treated Si(111) surface, the spectrum is dominated by the monohydride peak at 2080 cm^{-1}. As the surface was exposed to air with a relative humidity of 40% for several hours, the 2250 cm^{-1} peak due to intermediate oxidation, $SiH(O_3)$, appeared. Since there was no indication of the $SiH(SiO_2)$ peak at 2200 cm^{-1}, species with only one or two oxygen atoms inserted in the Si-Si back bonds must be unstable and rapidly converted to $SiH(O_3)$. After 7 hours of exposure to air, the Si-H mode almost completely disappeared, suggesting that oxidation had occurred over the entire surface.

To complement this information, studies with Si-H surfaces placed in dry oxygen ambient or in a desiccator with a relative humidity of 10% were performed. The oxidation of the Si-H bond on a Si(111)-H surface was significantly retarded in the low humidity environment as the $SiH(O_3)$ peak persisted for a longer period of time and had a greater intensity than for the studies in moist air. After 35 days of exposure, a broad Si-H vibration frequency was still observed and the $SiH(O_3)$ peak was strong. The same trend was recorded for Si(100)-H surfaces, so this result gives evidence that water is predominantly involved in Si-H bond oxidation. The Si(100)-H surface exposed to dry O_2

behaved in the same manner as one exposed to low humidity, suggesting that oxygen molecules are responsible for surface oxidation in the absence of moisture. Niwano et al. [25] concluded that water is crucial to the initial stages of surface oxidation of hydrogen terminated silicon. Their proposed mechanism involves water attacking the Si-H bond and oxygen molecules preferentially inserting into the back bonds of the surface silicon atoms, as implied by the enhanced $SiH(O_3)$ IR peak in the low humidity studies. This is in agreement with Miura et al. [29] who stated that water reacts more easily with the Si-H bond than oxygen does. They also suggested that the formation of oxygen-related bonds on the surface forces a shift from hydrophobicity to hydrophilicity, thus promoting further attack.

Quantum chemical studies of hydrogen terminated Si(111) performed by Teraishi et al. [31] used molecular orbital calculations and cluster models to trace the insertion of up to five oxygen atoms into the Si-Si bonds of the (111) surface. The first oxygen preferentially attacks the topmost layer. The second oxygen can either insert so that both oxygens are bound to a surface silicon atom with hydrogen termination or so that both oxygens are bound to a subsurface silicon atom. The latter configuration is favored. The third oxygen atom is most stable in the interbilayer position because it escapes the large strain caused by three insertions in the same plane. This suggests that inner Si-Si bonds are oxidized prior to the complete oxidation of the first bilayer. The fourth insertion occurs so that four oxygens coordinate the subsurface silicon atom. At this point, the oxide island will grow from this site along the lateral direction as the fifth oxygen preferentially inserts into a surface Si-Si bond adjacent to an atom that is already

coordinated to oxygen. This promotes aggregation rather than uniform distribution of oxygen.

Baierle and Caldas [32] performed quantum chemical calculations using the Modified Neglect of Diatomic Overlap in the Austin Model version (MNDO/AM1) to study the oxidation of the Si(111)-H surface. Their model is designed to accurately describe geometrical features of molecules, including vibrational frequencies and formation energies. Several conclusions were drawn from the parameterizations. Oxygens absorbed interstitially in Si-Si back bonds were more stable than as surface Si-OH terminations, which is clearly supported by experimental results. In agreement with Teraishi et al. [31], subsurface oxygen insertions tended to cluster together forming islands on the first layer and oxide growth proceeded laterally rather than vertically. Baierle and Caldas [32] stated that oxygen atoms do not insert more deeply into the substrate while there are open positions left in the first subsurface layer because migration to the second layer is not energetically favored. This point is the main contrast between the two computational studies.

1.7. Motivation to study Si(111)-H and other modified surfaces

Si(111)-H can now be reproducibly prepared to obtain an atomically flat surface with ideal termination of all the dangling bonds [13]. It has been demonstrated that this substrate is an excellent precursor for covalent linkage of alkyl chains on the surface [12,19,22]. These chemical modification studies lead the way toward tailor-made

monolayers that combine organic functionality with semiconductors. By fine-tuning the chemical properties of these surfaces, applications, such as those that would integrate biologically active species, can be realized.

Hydrogen terminated Si(111) also represents a good model to study surface reactivity with oxygen. Silicon is the basic substrate for semiconductor chips and microelectronic devices. Control of the surface oxidation and chemical passivation to remove dangling bonds are important issues that need to be addressed. By using nonlinear optics to probe the chemistry of Si(111)-H, there is promise that a relationship between the surface oxidation mechanism and the surface second-harmonic response can be elucidated.

References

1 Shen, Y. R., Nature **337**, 519 (1989)

2 Corn, R. M. and Higgins, D. A., Chem. Rev. **94**, 107 (1994)

3 Giordmaine, J. A., Sci. Amer. **210**, 38 (1964)

4 Franken, P. A., Hill, A. E., Peters, C. W. and Weinreich, G., Phys. Rev. Lett. **7**, 118 (1961)

5 Brown, F., Parks, R. E. and Sleeper, A. M., Phys. Rev. Lett. **14**, 1029 (1965)

6 Bloembergen, N., Appl. Phys. B **68**, 289 (1999)

7 Shen, Y. R., J. Vac. Sci. Technol. B **3**, 1464 (1985)

8 Saleh, B. E. A. and Teich, M. C., Fundamentals of Photonics, ch.15; John Wiley and Sons Inc. (1991)

9 Serway, R. A., Physics for Scientists and Engineers with Modern Physics, ch.43; 3rd Ed., Saunders College Publishing (1990)

10 Hilirichs, G., Gräf, D., Marowsky, G., Roders, O., Schnegg, A. and Wagner, P., J. Electrochem. Soc. **141**, 3145 (1994)

11 Sipe, J. E., Moss, D. J. and van Driel, H. M., Phys. Rev. B **35**, 1129 (1987)

12 Boukherroub, R., Morin, S., Bensebaa, F. and Wayner, D. D. M., Langmuir **15**, 3831 (1999)

13 Higashi, G. S., Chabal, Y. J., Trucks, G. W. and Raghavachari, K., Appl. Phys. Lett. **56**, 656 (1990)

14 Trucks, G. W., Raghavachari, K, Higashi, G. S. and Chabal, Y. J., Phys. Rev. Lett. **65**, 505 (1990)

15 Ubara, H., Imura, T. and Hiraki, A., Solid State Commun. **50**, 673 (1984)

16 Ulman, A., Chem. Rev. **96**, 1533 (1996)

17 Henry de Villeneuve, C., Pinson, J., Bernard, M. C. and Allongue, P., J. Phys. Chem. B **101**, 2415 (1997)

18 Terry, J., Mo, R., Wigren, C., Cao, R., Mount, G., Pianetta, P., Linford, M. R. and Chidsey, C. E. D., Nucl. Instr. and Meth. in Phys. Res. B **133**, 94 (1997)

19 Linford, M. R. and Chidsey, C. E. D., J. Am. Chem. Soc. **115**, 12631 (1993)

20 Linford, M. R., Fenter, P., Eisenberger, P. M. and Chidsey, C. E. D., J. Am. Chem. Soc. **117**, 3145 (1995)

21 Wagner, P., Nock, S., Spudich, J. A., Volkmuth, W. D., Chu, S., Cicero, R.L., Wade, C. E., Linford, M. R. and Chidsey, C. E. D., J. Struct. Biol. **119**, 189 (1997)

22 Boukherroub, R., Morin, S., Sharpe, P., Wayner, D. D. M. and Allongue, P., Langmuir (2000) in press

23 Takahagi, T., Ishitani, A., Kuroda, H., Nagasawa, Y., Ito, H. and Wakao, S., J. Appl. Phys. **68**, 2187 (1990)

24 Morita, M., Ohmi, T., Hasegawa, E., Kawakami, M. and Ohwada, M., J. Appl. Phys. **68**, 1272 (1990)

25 Niwano, M., Kageyama, J., Kurita, K., Kinashi, K, Takahashi, I. and Miyamoto N., J. Appl. Phys. **76**, 2157 (1994)

26 Kato, Y., Ito, T. and Hiraki, A., Jpn. J. Appl. Phys. **27**, L1406 (1988)

27 Neuwald, U., Hessel, H. E., Feltz, A., Memmert, U. and Behm, R. J., Appl. Phys. Lett. **60**, 1307 (1992)

28 Angermann, H., Henrion, W., Rebien, M., Fischer, D., Zettler, J. -T. and Röseler, A., Thin Solid Films, **313-314**, 552 (1998)

29 Miura, T., Niwano, M., Shoji, D. and Miyamoto, N., Appl. Surf. Sci. **100/101**, 454 (1996)

30 Sieger, M. T., Luh, D. A., Miller, T. and Chiang, T. -C., Phys. Rev. Lett. **77**, 2758 (1996)

31 Teraishi, K., Takaba, H., Yamada, A., Endou, A., Gunji, I., Chatterjee, A., Kubo, M., Miyamoto, A., Nakamura, K. and Kitajima, M., J. Chem. Phys. **109**, 1495 (1998)

32 Baierle, R. J. and Caldas, M. J., Intl. J. Modern Phys. B **13**, 2733 (1999)

2. Theory

2.1. Distinction between linear and nonlinear optics

The basic difference between linear and nonlinear optics is what happens to the frequency of light as it is transmitted through or reflected from a medium. In linear optics, there is no change in the frequency. In nonlinear optics, harmonics of the fundamental frequency are generated. When a beam of sunlight is passed through a prism, a rainbow is observed, illustrating the phenomenon of refraction. Reflection and absorption are also everyday linear optical occurrences with common light sources. When in the presence of an intense electric field, matter does not respond in the same manner, leading to nonlinear optical effects [1].

The Lorentzian dipole model describes light as it passes through a dielectric medium. It approximates the bonding of electrons to nuclei as charged particles attached by springs to nuclei [2]. The light wave is an oscillating electric field and the medium's atoms are dipoles. If the irradiance (power per square meter) is not intense, a polarization is induced in the atomic dipoles, which is linear in the amplitude of the incident electric field, so they are harmonically driven. The polarization is essentially a redistribution of negative charge. For a given atom, the nucleus is too heavy to be affected by the light wave's electric field, and the inner shell electrons are too tightly bound. However, the valence electrons can be rearranged because they are more weakly bound, either shared among atoms in a covalent medium or transferred from an electron-rich atom to an electron-poor

atom in an ionic medium [3]. Nonlinearity is introduced when the irradiance is significantly intense enough that it approaches the magnitude of the electric field in the medium [1], which keeps the nuclei and electrons in an equilibrium state. In this case, the resulting polarization is not proportional to the electric field of the light wave because the redistribution of electrons is too extensive for the atom to return to its equilibrium state. The induced oscillation of the atomic dipoles is then complex and includes a component at the second harmonic of the fundamental electric field.

As described in the Introduction, nonlinear materials are noncentrosymmetric. Due to the lack of a center of symmetry, an incident electric field can polarize the medium more efficiently in one direction than the other, creating an unequal distribution of negative charge. The resultant distorted polarization wave is the sum of three components: a wave at the fundamental frequency, a wave at the second-harmonic frequency and a steady polarization, [3] as shown in Figure 2.1.1. In this example, the intense field in the 'positive' direction does not polarize the medium as much as the field in the 'negative' direction, so the lobes are larger for the negative values of the oscillation.

The interaction of an electromagnetic (EM) field of optical frequency, ω with condensed matter can be described in terms of a general polarization amplitude, $P(\omega, 2\omega,\ldots)$, induced by the field of amplitude $E(\omega)$

$$P(\omega,2\omega,\ldots) = \varepsilon_0 \left[\chi^{(1)}(\omega)E(\omega) + \chi^{(2)}(\omega,2\omega)E^2(\omega) + \ldots\right] \qquad 2.1.1$$

where $\chi^{(i)}$ is the ith order dielectric susceptibility tensor describing the material response and ε_0 is the permittivity of free space. The first term on the right-hand side of the

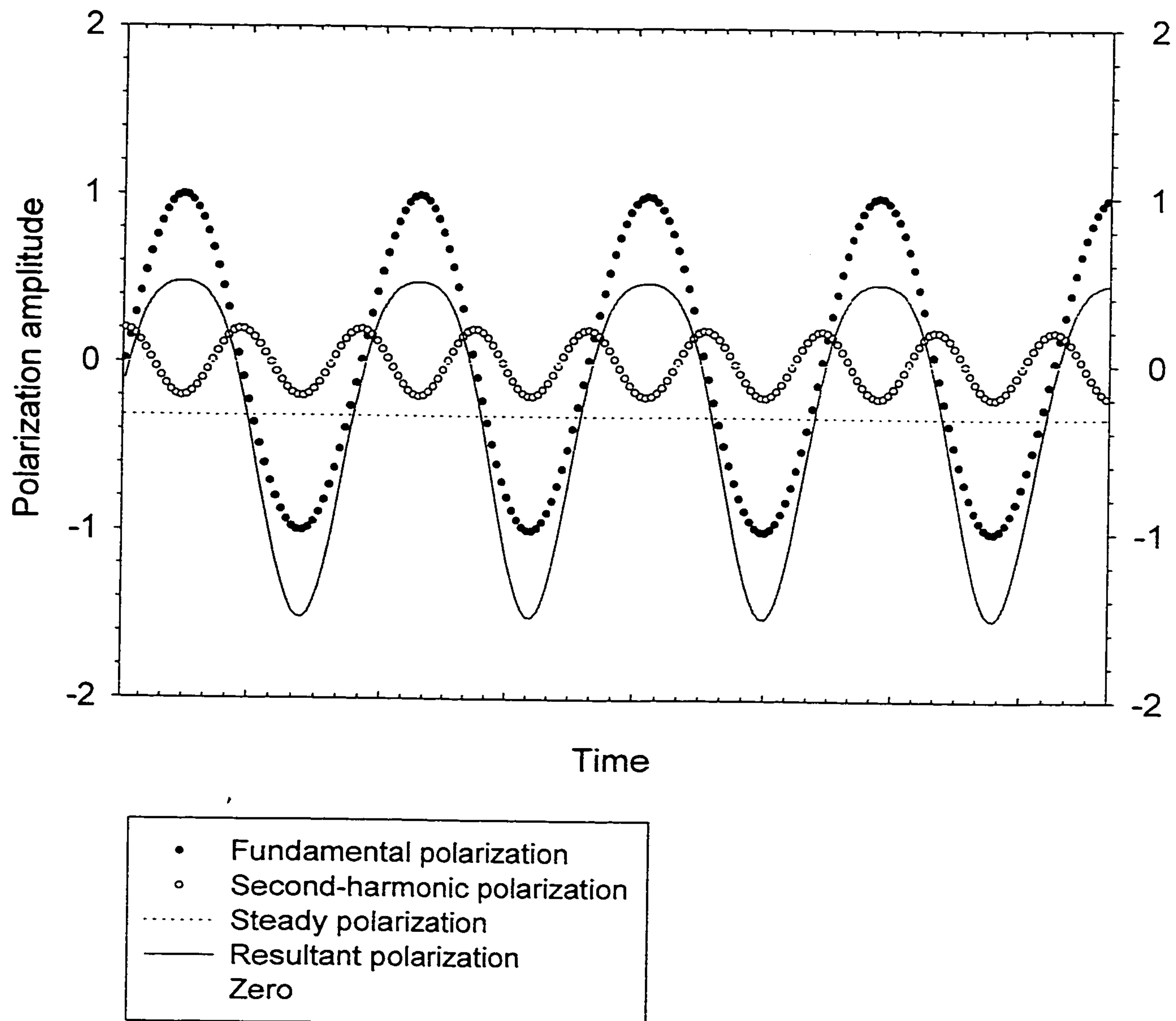

Figure 2.1.1 Analysis of a nonlinear polarization wave

equation describes the linear optical response. As described above, the higher-order terms are nonlinear and only become significant at high EM field strengths. The second term in equation 2.1.1, with a polarization quadratic in the EM field, describes the lowest order nonlinear optical response responsible for SHG [4].

2.2. Optical probes

Purely optical probes possess a number of important advantages for the examination of surface properties. The time resolution available from laser-based probes is excellent, with the advent of systems that can produce femtosecond pulses. The broad spectral bandwidth and tunability of laser sources also have played a role in making optical techniques a preferred method to determine surface structure, detect monolayer adsorption or monitor reactions *in situ*. They can be used for any interface that is transparent to a fundamental wavelength of light as well as the frequency-doubled radiation, so buried interfaces are not excluded. Experimental conditions are flexible, as it is not necessary for samples to be held in ultra-high vacuum; ambient air does not pose a problem. Most of all, optical probes are non-destructive, so samples can be analyzed repeatedly or constantly, as the experiment requires.

The main challenge for optical techniques is obtaining a sufficient degree of interface sensitivity. Only the first few atomic layers of a medium generate the surface response; however, light can penetrate a material to a substantial depth. Consequently, it is essential for the optical probe to possess a means of suppressing the bulk response [5]. Traditional

spectroscopic methods, such as absorption, emission and Raman scattering, are generally not able to distinguish signals as originating from the bulk or from the surface [6].

When used to probe the crystal structure of a centrosymmetric medium such as silicon, SHG is subject to a symmetry constraint that discriminates against the bulk signal. SHG can selectively probe such an interface without being overwhelmed by bulk contributions because second-order processes are electric-dipole forbidden in the bulk of centrosymmetric media, but this constraint is lifted at the interface. On the other hand, third-harmonic generation (THG), provided there are not any strong resonantly enhanced surface electric-dipole effects, is dominated by a bulk electric-dipole contribution, making it an excellent tool for probing the bulk structure [7]. Structural discontinuity and/or field discontinuity are responsible for a given surface's nonlinear behavior [8].

Structural discontinuity refers to the structural disparity between the surface layer and the ambient phase. In the experiments described here, the silicon bonds at the interface contribute to this parameter. However, a clean semiconductor surface with dangling bonds has an even larger contribution from structural discontinuity, due to the non-uniform electron density. Chemisorbed species bound to the dangling bonds quench this characteristic, lowering the SHG response [8]. Structural asymmetry, such as in the case of molecules self-assembled on a surface with a particular orientation, is another important consideration when evaluating the source of surface nonlinearity.

Field discontinuity depends on the gradient of the field across the interface [9]. In the case of Si(111), the dielectric constant (ε) is 12, while in air, ε = 1. This mismatch is reduced when there are adsorbates on the surface, as a hydrocarbon or oxide layer mediates the change in ε at the interface. For hydrogen-terminated Si(111), the thin monolayer does not alter the field gradient significantly, so the field discontinuity is considerable. In some cases, only one discontinuity is active. The surface structure is not very different from that in the bulk for a liquid surface, so field discontinuity makes the most important contribution to the nonlinear response [8]. On the other hand, if the dielectric constants of the two media are closely similar, the field becomes continuous across the interface; therefore, this contribution to the overall surface susceptibility tensor vanishes. However, if one medium is a solid and the other is a liquid, a strong structural discontinuity is still present [9].

The SHG signal from the surface is measured at fixed input and output polarizations as a function of azimuthal angle ϕ, where ϕ is determined relative to a particular crystalline axis on the surface. In the case of Si(111), the <01-1> direction was used. It is conventional to use the term *p-polarization* when the electric field is polarized parallel to the plane of incidence and *s-polarization* for light which is polarized perpendicular to the plane of incidence [10]. The plane of incidence refers to the laser beam's horizontal trajectory, which contains the surface normal. For the fundamental and second-harmonic beam pair in these experiments, a total of four polarization combinations is possible, as shown in Figure 2.2.1. Rotational anisotropy measurements at single-crystal surfaces were first demonstrated on Si(111) by Guidotti et al. [11,12] and by Shen and co-workers

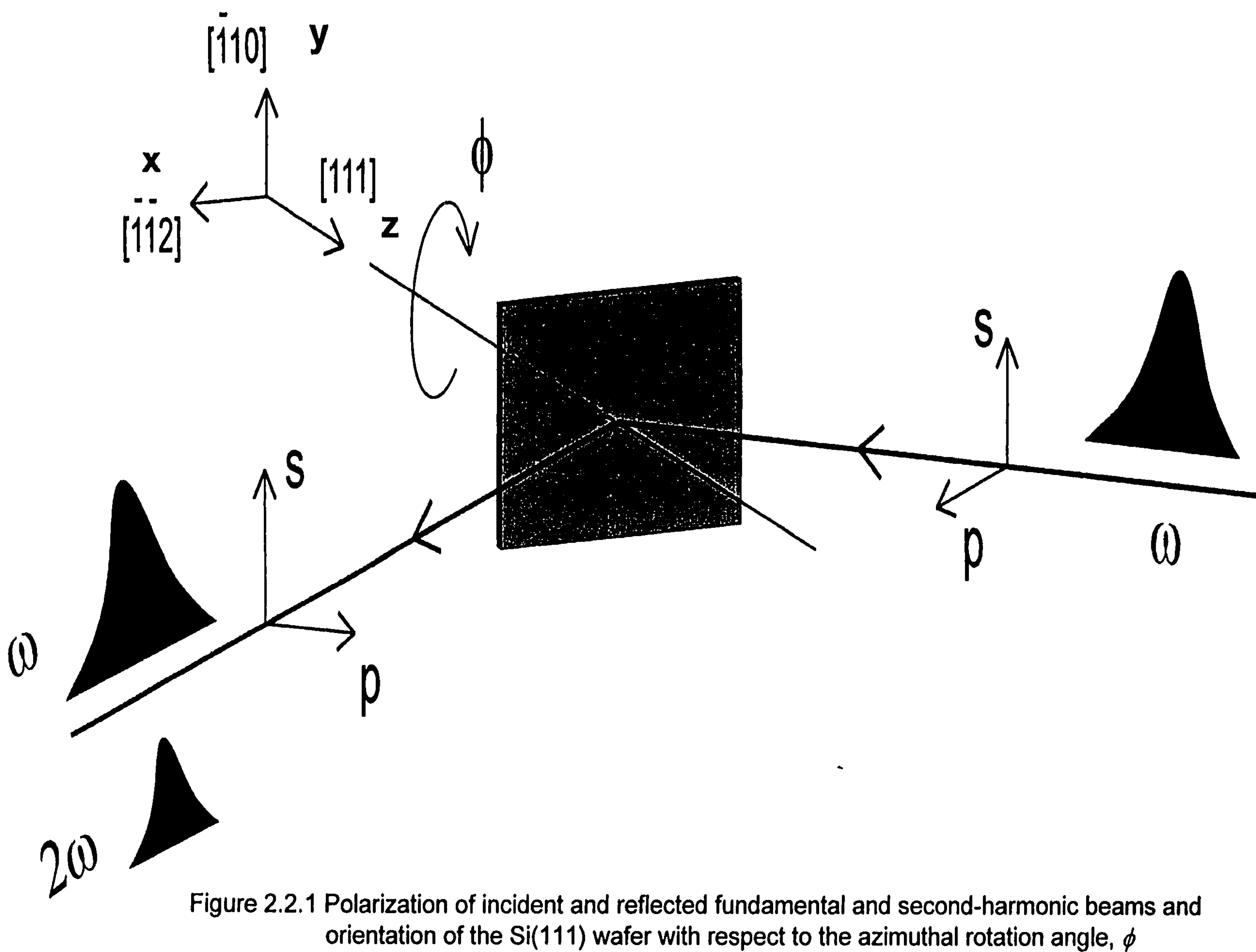

Figure 2.2.1 Polarization of incident and reflected fundamental and second-harmonic beams and orientation of the Si(111) wafer with respect to the azimuthal rotation angle, ϕ

[13,14]. The standard coordinate system (x,y,z) adopted for this type of measurement is as follows: x-z is taken as the plane of incidence with z normal to the crystal surface, and y is then normal to the plane of incidence. As the crystal rotates about the z-axis by a variable angle ϕ, the SHG intensity varies based on the symmetry of the second-harmonic tensor $\chi^{(2)}$, which is dependent on the crystal symmetry [11].

2.3. Harmonic generation at surfaces

2.3.1. SHG from a centrosymmetric cubic crystal

The phenomenological theory of SHG in reflection from silicon crystals has been described in detail in the literature [15]. The efficiency of SHG is governed by the second-order macroscopic nonlinear susceptibility tensor $\chi^{(2)}$ through the relation

$$P^{(2)}(2\omega) = \chi^{(2)} E(\omega) E(\omega) \qquad 2.3.1$$

For the Si(111) surface, the detailed form of $\chi^{(2)}$ has four independent nonzero elements: three that describe the isotropic component of the SHG response and one that governs the anisotropic component. In addition to these susceptibility elements that describe the electric-dipole response of the surface, the total nonlinear response has electric-quadrupole contributions from the bulk of the crystal as well. The isotropic and anisotropic contributions from the bulk are each described by a susceptibility. Altogether, there are six complex susceptibilities that are needed to fully describe the SHG response for the case of a Si(111) surface. It has been shown that the surface- and bulk-derived contributions can be combined in an effective $\chi^{(2)}$ tensor [15]. For the following

discussion of results, the surface response is understood to include both of these contributions.

2.3.2. Rotational anisotropy equations

The polarization combination for a given experiment is written so the first index refers to the fundamental frequency and the second to the second-harmonic frequency. SHG efficiencies for these polarization combinations are defined in terms of the intensities (I) of the fundamental and second-harmonic radiation as shown in equation 2.3.2 for the (s,p) case.

$$R_{sp} = \frac{I_p(2\omega)}{I_s(\omega)^2} \qquad 2.3.2$$

The rotational anisotropy of the SHG efficiency is described by equation 2.3.3.

$$\begin{aligned} R_{sp} &= |A_{sp} + B_{sp}\cos(3\phi)|^2 \\ &= |A_{sp}|^2 + |B_{sp}|^2\cos^2(3\phi) + 2|A_{sp}|\,|B_{sp}|\cos(3\phi)\cos(\theta_{sp}) \end{aligned} \qquad 2.3.3$$

ϕ is defined as the angle between the plane of incidence and a <2-1-1> direction on the (111) surface. The coefficient of the ϕ terms is 3 because of the threefold symmetry of the (111) surface, clearly evident in Figure 1.3.2a (page 7) as each surface atom is back-bonded to three subsurface atoms. For a (001) surface, there is fourfold symmetry, so the coefficient, in that instance, would be 4.

To simplify further discussion of the parameters of the SHG signal, equation 2.3.3 can be rewritten as equation 2.3.4,

$$R_{sp} = \alpha_{sp} + \gamma_{sp}\cos^2(3\phi) + \beta_{sp}\cos(3\phi) \qquad 2.3.4$$

such that $\alpha_{sp} = |A_{sp}|^2$,

$\gamma_{sp} = |B_{sp}|^2$

and $\beta_{sp} = 2|A_{sp}|\,|B_{sp}|\cos(\theta_{sp})$

θ_{sp} is the relative phase between A_{sp} and B_{sp}, as shown in equation 2.3.5. Only the absolute magnitude of θ_{sp} is known, but not its sign because A_{sp} and B_{sp} are complex-valued and by taking the square of the absolute value of these parameters, this information is lost.

$$\frac{A_{sp}}{B_{sp}} = \frac{|A_{sp}|}{|B_{sp}|}\exp(i\theta_{sp}) \qquad 2.3.5$$

Similar expressions (equations 2.3.6 – 2.3.8) hold for the SHG efficiencies R_{pp}, R_{ps}, and R_{ss}, except that an isotropic response is not present for s-polarized second-harmonic radiation.

$$R_{pp} = \alpha_{pp} + \gamma_{pp}\cos^2(3\phi) + \beta_{pp}\cos(3\phi) \qquad 2.3.6$$

$$R_{ps} = \gamma_{ps}\sin^2(3\phi) \qquad 2.3.7$$

$$R_{ss} = \gamma_{ss}\sin^2(3\phi) \qquad 2.3.8$$

The isotropic and anisotropic parameters in equations 2.3.3-2.3.8 are related to the six surface and bulk microscopic nonlinear susceptibilities of Si(111) [15]. In practice, one uses the equation pertinent to the polarization combination in a given experiment to calculate α, γ and θ. The square root of α obtains A and the square root of γ obtains B. In the discussion of results, the polarization combination is specified, but subscripts are omitted for the sake of simplicity.

The Si(111) surface, as described above, has threefold symmetry, so a threefold symmetric pattern is expected for the second-harmonic radiation as a function of rotation of the sample about its surface normal. Figure 2.3.1 illustrates the characteristic rotational anisotropy plot for (p,p) or (s,p) polarization combination. The three large lobes and three smaller lobes, shown as a solid line, are the sum of the $\cos(3\phi)$ function, the $\cos^2(3\phi)$ function and the isotropic term, α, all shown as dotted lines. The lack of an isotropic term for s-polarized second-harmonic radiation changes the appearance of the rotational anisotropy plot for the (p,s) polarization combination. Six identical lobes are observed in this case, derived solely from the $\sin^2(3\phi)$ function with its coefficient, γ.

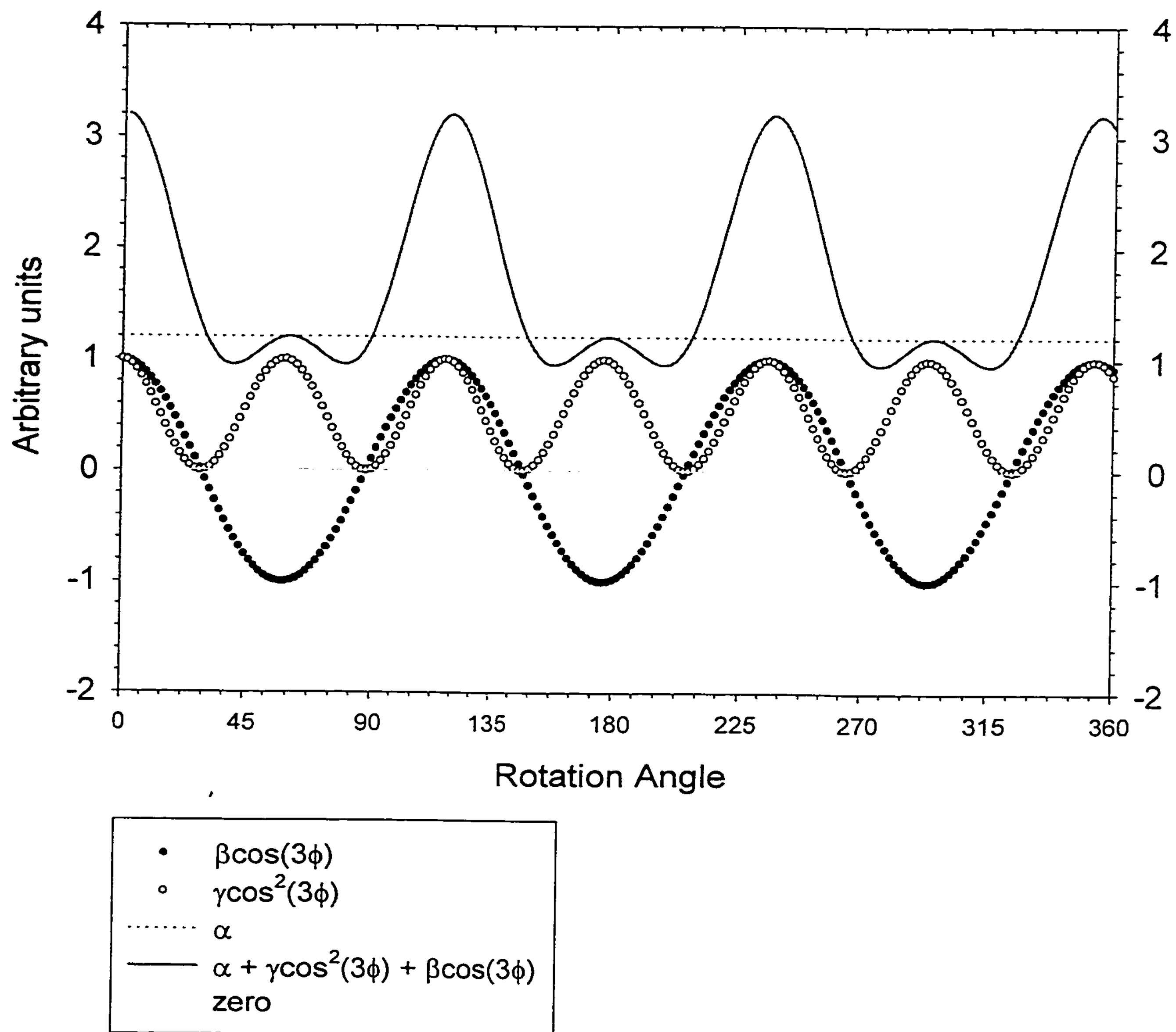

Figure 2.3.1 Contributions to the second-harmonic signal for Si(111), refer to equation 2.3.6

References

1 Higgins, T. V., "Nonlinear optical effects are revolutionizing electro-optics" Laser Focus World, August 1994, p.67-74

2 Prasad, P. N. and Williams, D. J., Introduction to Nonlinear Optical Effects in Molecules and Polymers, ch.2; John Wiley and Sons Inc. (1991)

3 Giordmaine, J. A., Sci. Amer. **210**, 38 (1964)

4 McGilp, J. F., J. Phys. D: Appl. Phys. **29**, 1812 (1996)

5 Reider, G. A. and Heinz, T. F., "Second-order nonlinear optical effects at surfaces and interfaces: Recent advances" in Photonic Probes of Surfaces, ch.9; Halevi, P., Ed.; Elsevier Science (1995)

6 Eisenthal, K. B., Chem. Rev. **96**, 1343 (1996)

7 Bottomley, D. J., Lüpke, G., Mihaychuk, J. G. and van Driel, H. M., J. Appl. Phys. **74**, 6072 (1993)

8 Shen, Y. R., Nature **337**, 519 (1989)

9 Guyot-Sionnest, P., Chen, W. and Shen, Y. R., Phys. Rev. B **33**, 8254 (1986); Guyot-Sionnest, P. and Shen, Y. R., Phys. Rev. B **35**, 4420 (1987)

10 Hopf, F. A. and Stegeman, G. I., "Linear Optics" vol.1 of Applied Classical Electrodynamics, ch.11; John Wiley and Sons Inc. (1985)

11 Driscoll, D. and Guidotti, D. A., Phys. Rev. B **28**, 1171 (1983)

12 Guidotti, D., Driscoll, T. A. and Gerritsen, H. J., Solid. State Commun. **46**, 337 (1983)

13 Tom, H. W. K., Heinz, T. F. and Shen, Y. R., Phys. Rev. Lett. **51**, 1983 (1983)

14 Heinz, T. F., Loy, M. M. T. and Thompson, W. A., Phys. Rev. Lett. **54**, 63 (1985)

15 Sipe, J. E., Moss, D. J. and van Driel, H. M., Phys. Rev. B **35**, 1129 (1987)

3. Experimental

3.1. Second-harmonic generation

Second-harmonic generation (SHG) was monitored in reflection from Si(111) samples cut from wafers purchased from Virginia Semiconductor. The n-type (phosphorus dopant) Cz-silicon wafers had a resistivity of 1.16-3.04 Ωcm and a miscut of less than 0.5°. In all experiments, except those conducted in a nitrogen purge environment, the sample was exposed to air during the measurements. The wafer shard was mounted in such a way that it could be rotated 360° about its surface normal, with the incident laser beam at 45° in a horizontal plane. The zero of the azimuthal rotation angle was such that a <01-1> direction was perpendicular to the plane of incidence. The particular <01-1> direction was selected with reference to the primary flat on the single batch of wafers.

Laser pulses with a central wavelength of 830 nm and a duration of ~80 fs were obtained from the output of a 1 kHz Ti:sapphire regenerative amplifier (Positive Light), seeded with the output of a solid-state pumped femtosecond Ti:sapphire oscillator (Spectra-Physics). Spectra of the laser pulses were nearly Gaussian with full width at half-maximum of ~13 nm. The laser beam, with a pulse energy of ~3μJ at 1 kHz repetition rate, was focused on the sample by using a 100 cm focal length lens. A Berek's polarization compensator and a Glan-laser polarizer were used to select the plane of polarization of the incident laser beam, and a second polarizer was used to select the polarization of the reflected second-harmonic light. The second harmonic was separated

from reflected fundamental light and generated higher-harmonic light, by using a Pellin-Broca prism and colored glass filters and detected with a photomultiplier tube (PMT). A glass filter, placed just before the sample, removed second-harmonic radiation from the incident laser beam. The signal from the PMT was averaged by boxcar integration and displayed with a personal computer. All data was then transferred to a graphing software program for analysis and interpretation.

A small fraction of the incident laser beam was split off and used for SHG by transmission through a quartz waveplate. This reference signal was recorded simultaneously with the SHG signal from the sample and used for normalization against variations in laser pulse energy or duration. It was confirmed that the SHG signal was quadratic in the laser fluence, by using a neutral density filter, as shown in Figure 3.1.1.

3.1.1. Pellin-Broca prism

The Pellin-Broca prism is a constant-deviation dispersing prism. It is ideally used in spectroscopic configurations where the detection of several wavelengths, independently, is desirable. One can conveniently mount the light source at a fixed angle and rotate the prism to look at a particular wavelength without moving the detection system. The Pellin-Broca prism can be decomposed into two 30° right prisms and one 45° right prism, as shown in Figure 3.1.2 [1]. If a ray of wavelength λ_1 traverses the component prism DAE symmetrically and is then reflected at 45° from face AB; the ray will emerge from face DC having experienced a total deviation of 90°. If the prism is rotated slightly about an axis normal to the paper, the incoming beam will have a new incident angle; therefore, a

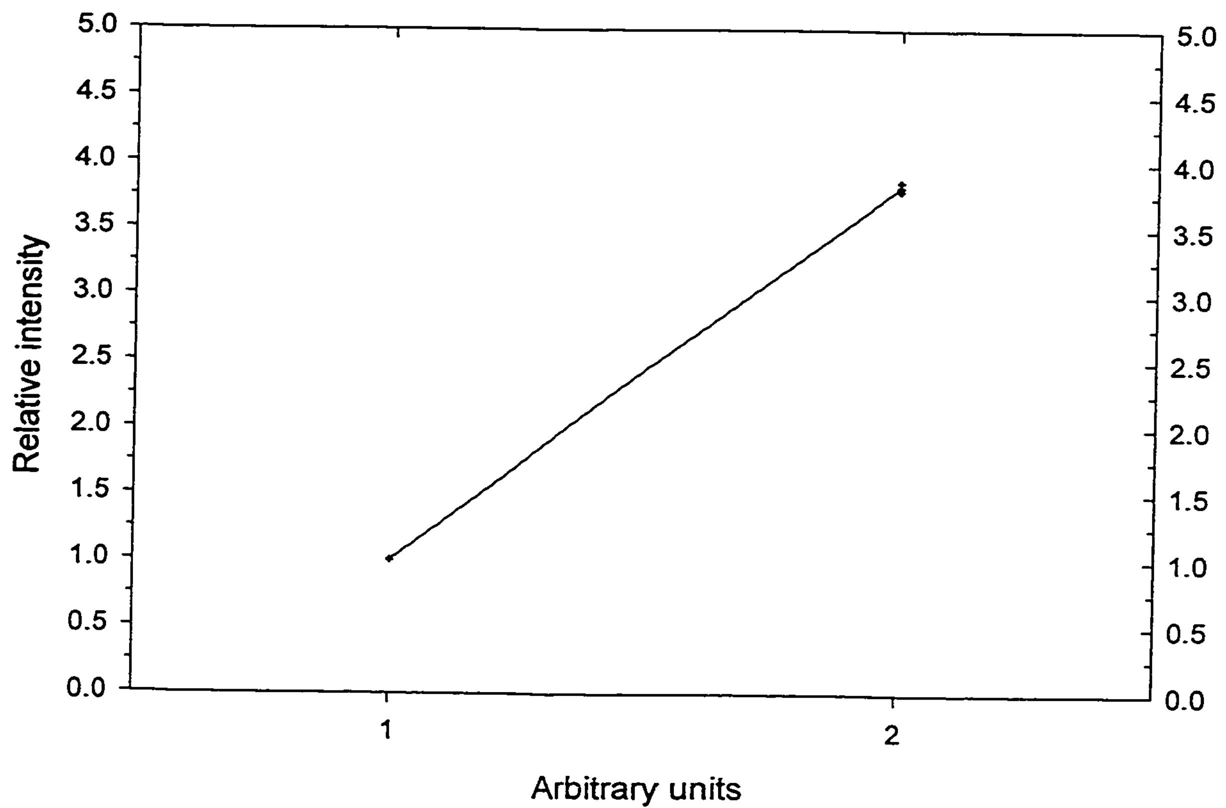

Figure 3.1.1 SHG signal intensity with and without a 46% neutral density filter to attenuate the maximum pulse energy of ~3.0 μJ

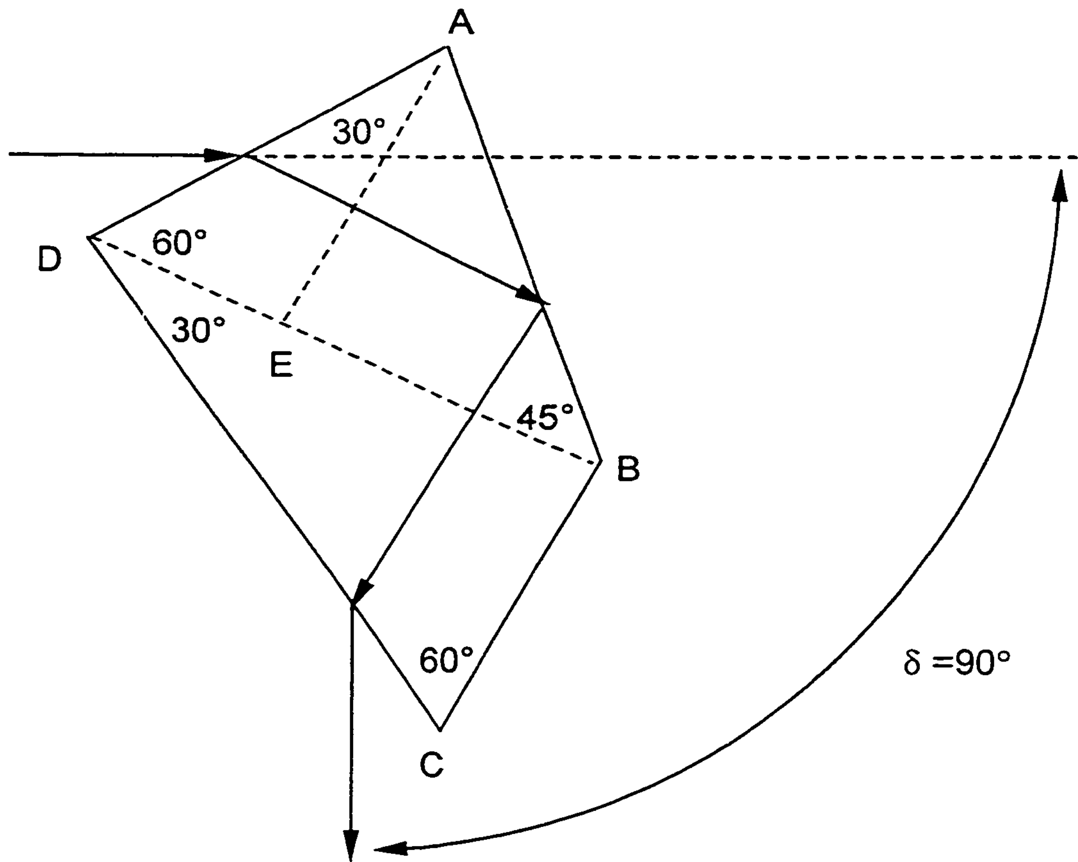

Figure 3.1.2 Pellin-Broca prism

different wavelength, λ_2 will now undergo a minimum deviation of 90° [1]. To determine the location of the pivot point, the length of face DC is measured and a circle of radius $DC/\sqrt{2}$ is inscribed on the prism mount. This circle is concentric with the mount's axis of rotation; the prism is placed inside the circle with face DC as a chord and the pivot point falls directly over the axis of the mount [2].

For incident radiation at 830 nm, the indices of refraction (*n*) in fused silica, for the fundamental, second- and third-harmonic wavelengths, used to calculate the incident angle (θ_i) are shown in the table below.

λ (nm)	$n^{\dagger}$	θ_i (deg)
830.0	1.45288	46.59
632.8	1.45705	46.76
415.0	1.46865	47.25
276.6	1.49544	48.39

† from Handbook of Optical Constants of Solids, Palik, E.D., Ed.; Academic Press Inc. (1985)

Using Snell's Law, the angle of refraction from the air-fused silica interface must be 30° to allow minimum deviation of the incident beam. The HeNe wavelength (632.8 nm) is also included in the table as this beam was used for alignment purposes in the experimental set-up.

3.2. Experimental conditions

3.2.1. Third-harmonic generation

For the experiments where third-harmonic generation (THG) was recorded, appropriate colored glass filters were used to exclude the fundamental and second-harmonic light before detection by the PMT. Otherwise, the apparatus set-up was identical. When SHG and THG from the z-cut quartz sample were monitored, it was mounted such that its position, with respect to the incident laser beam, was the same as that used for the Si(111) samples.

3.2.2. Nitrogen purge

For the experiments conducted in a nitrogen purge environment, a Plexiglas box was cut to fit over the sample mount. In order to exclude oxygen and moisture as much as possible, it had an inlet for continuous dry nitrogen flow. It had perforations to permit the entry of the incident beam and exit of the reflected laser beam during measurement of the rotational anisotropy plots.

3.2.3. Ultraviolet irradiation

A mercury-argon pen lamp (model 6035) from Oriel Instruments was used as the ultraviolet source for photo-oxidation of the hydrogen terminated Si(111) surfaces. The lamp was used without a filter for the 254-nm irradiation and, with a long wave conversion filter (model 6042), for 350-nm broadband irradiation. The distance from the

center of the lamp fixture to the surface of the sample was either 10 cm or 15 cm for most experiments and the irradiance in each case was calculated from published specifications [3].

The data acquisition program was modified to allow continuous monitoring of the signal over long periods of time. Parameters were devised to acquire data over 10, 12.5 or 25 minutes. The stepper motor was turned off so the sample did not rotate.

3.3. Preparation of samples

Native oxide samples were cut from as-received wafers and sonicated in Milli-Q water for five minutes. Excess water was removed with pressurized nitrogen and the samples were dried in air. Hydrogen terminated Si(111) samples were prepared by cleaning in 3:1 concentrated H_2SO_4 / 30% H_2O_2 at 100°C for 20 minutes, followed by copious rinsing with Milli-Q water. The surfaces were etched with clean room grade 40% aqueous deoxygenated NH_4F for 15 minutes [4] and transferred, without rinsing, onto the sample mount. For the preparation of a decyl monolayer on Si(111), the Si(111)-H was transferred into a Schlenk tube containing 10 ml of deoxygenated decylmagnesium bromide (1.0M solution in diethyl ether) and warmed to 85°C for 16 hours [5]. The surface was then rinsed at room temperature with 1% CF_3COOH solution in THF, Milli-Q water and finally trichloroethane. The decyloxy monolayer on Si(111) was prepared by reaction of Si(111)-H in deoxygenated neat decanol or decanal for 16 hours at 85° [6]. All cleaning and etching reagents were clean room grade and supplied by Amplex. All

other reagents were obtained from Aldrich and were of the highest purity available. Dr. Rabah Boukherroub, a research associate at NRC, performed all of the chemical modifications of the Si(111) surfaces.

References

1 Hecht, E., Optics, ch.5; 2nd Ed., Addison-Wesley (1987)

2 McClain, W. M., Appl. Optics **12**, 1405 (1973)

3 Reader, J., Sansonetti, C. J. and Bridges, J. M., Appl. Optics **35**, 78 (1996)

4 Wade, C. P. and Chidsey, C. E. D., Appl. Phys. Lett. **71**, 1679 (1997)

5 Boukherroub, R., Morin, S., Bensebaa, F. and Wayner, D. D. M., Langmuir **15**, 3831 (1999)

6 Boukherroub, R., Morin, S., Sharpe, P., Wayner, D. D. M. and Allongue, P., Langmuir (2000) in press

4. Results and Discussion

4.1. Influence of a center of inversion upon harmonic response

SHG is governed by $\chi^{(2)}$, the second-order nonlinear susceptibility tensor and THG is governed by $\chi^{(3)}$, the third-order nonlinear susceptibility tensor. These nonlinear optical responses from a centrosymmetric medium, such as Si(111) are not of the same order of magnitude as those from a noncentrosymmetric medium, such as z-cut quartz, as illustrated in Figures 4.1.1 and 4.1.2.

Silicon is centrosymmetric. In the bulk of such a material, by symmetry, a second-order nonlinear response is forbidden, so $\chi^{(2)}$ is zero. At the surface, the center of inversion is removed and $\chi^{(2)}$ becomes nonzero, due to the surface specific signal present. $\chi^{(3)}$ is always electric-dipole allowed in the bulk for centrosymmetric media, while $\chi^{(2)}$ is allowed only because the lack of translational symmetry across the interface relaxes the symmetry constraint [1]. Consequently, $\chi^{(2)}$ is expected to have an intrinsically smaller value than $\chi^{(3)}$. $\chi^{(3)}$ derives its magnitude from the sum of a surface and a bulk component, but the latter dominates because of the much larger (typically > 10^2) volume of sample contributing [2]. The large contrast in the measured response for SHG and THG of Si(111), shown in Table 4.1.1, can be explained by this difference in origin for each of the two nonlinear responses.

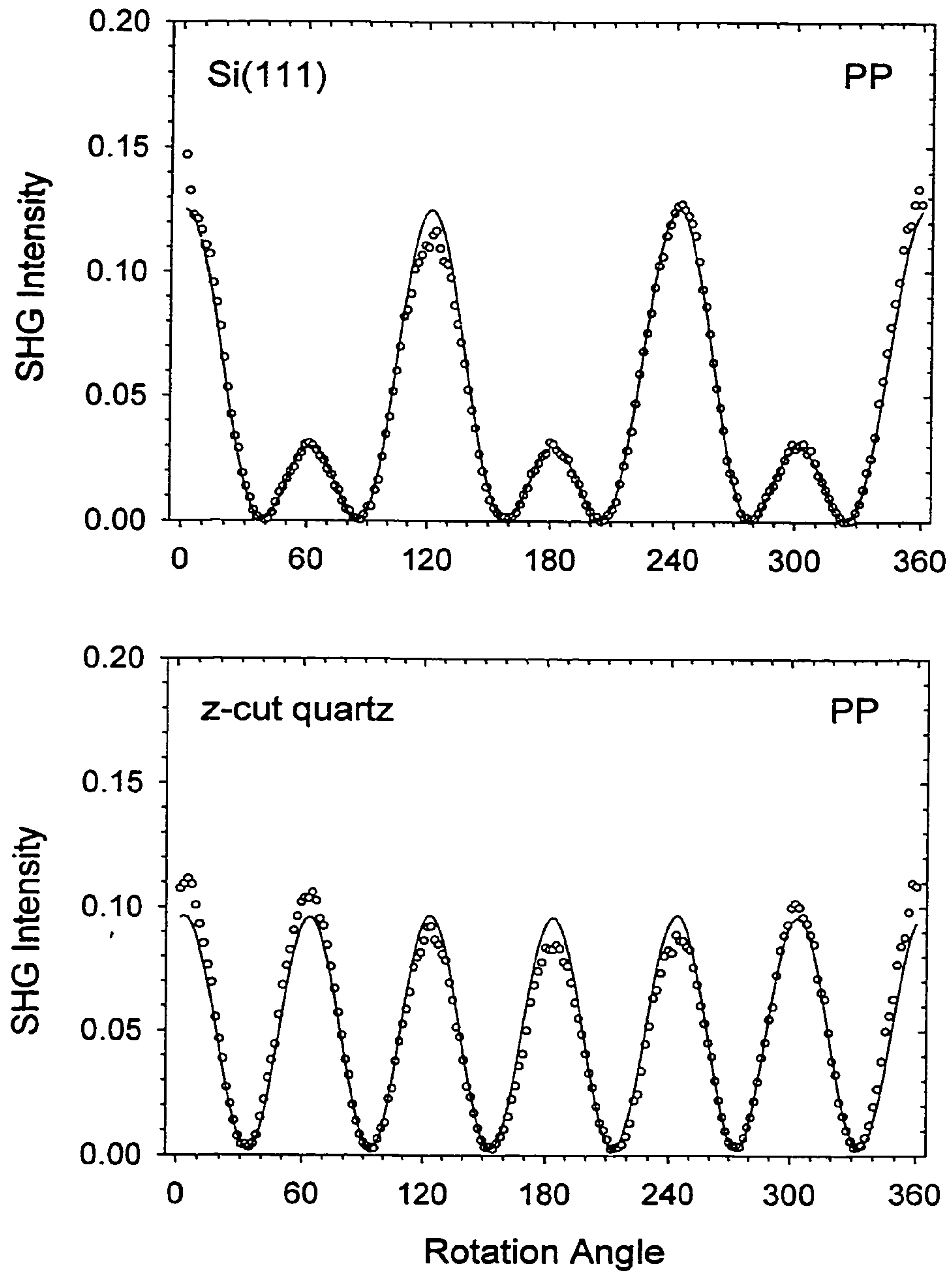

Figure 4.1.1 Comparison of second-harmonic signal

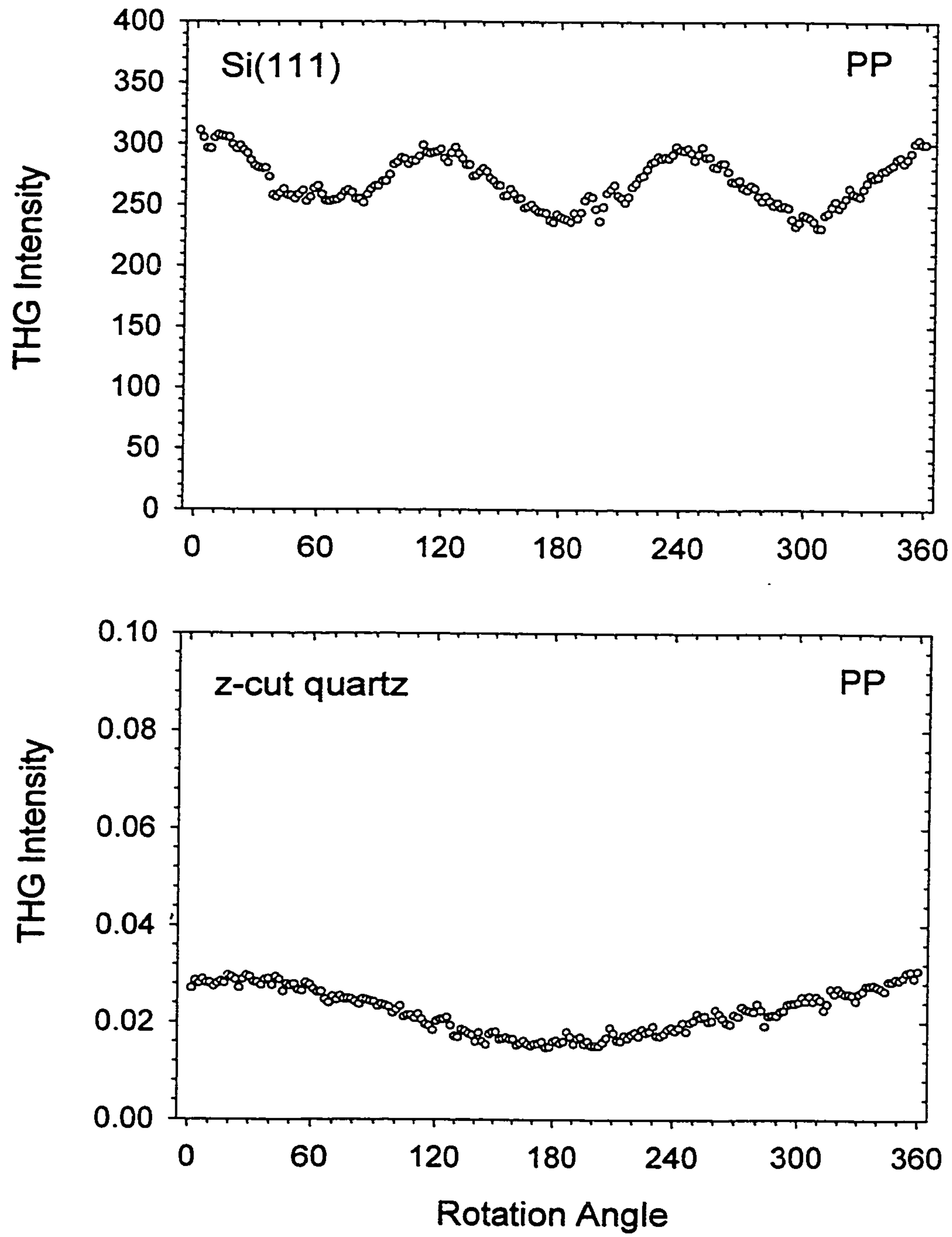

Figure 4.1.2 Comparison of third-harmonic signal

	$\chi^{(2)}$	$\chi^{(3)}$
Si(111)	0.13	300
z-cut quartz	0.09	0.03

Table 4.1.1 Comparison of the second- and third-harmonic responses of centrosymmetric and noncentrosymmetric media

Z-cut quartz is noncentrosymmetric. The z-axis is normal to the surface and parallel to the optic axis. No isotropic component is present in the second-order response, so six lobes of equal intensity are observed for SHG. The lack of a center of inversion in z-cut quartz means that this material does not have a surface specific response for SHG. Contributions from the bulk are not suppressed. Similarly, THG has a surface and a bulk component; however, the signal intensity from a noncentrosymmetric medium for THG is generally much weaker than for SHG since THG is a higher order process [3]. The values obtained in Table 4.1.1 follow this general rule, but it might have been expected that the THG signal would be more than three times smaller than the SHG response.

The dielectric constant for silicon is 12, while that for z-cut quartz is ~ 4. A higher dielectric constant makes a material more polarizable, which, in turn, leads to an increase in its nonlinear response. The comparison between the THG signals for the two media is striking. The response from Si(111) is four orders of magnitude larger than the response from z-cut quartz. There is not a very significant difference between the values obtained for SHG, which may be due to the fact that $\chi^{(2)}$ for Si(111) is a surface specific response,

while $\chi^{(2)}$ for z-cut quartz has contributions from the bulk. In silicon, the escape depth for the second-harmonic light is ~ 100Å, yet the surface region represents at most 10Å.

4.2. Comparison of chemically modified Si(111) surfaces

The effect of chemical modification on a Si(111) surface can be anticipated from the following simple model, in which the surface SHG response is associated with the network of Si-Si back bonds at the interface. In the bulk of the silicon crystal, the Si-Si bonds are centrosymmetric and therefore inactive in SHG. However, covalent bonding of foreign species to the surface silicon atoms makes a difference. Figure 1.3.2b (page 7) illustrates how hydrogen terminates every bond that is normal to the surface to yield a Si(111)-H monolayer. The proximity of the foreign species to the Si-Si back bonds that are connected to the surface silicon atoms induces a polarization in these bonds, making them active in SHG.

Substitution of more electronegative foreign species causes greater polarization of the Si-Si back bonds and should lead to an enhancement of the SHG response. Therefore, an increase in SHG efficiency with electronegativity of the surface species, from hydrogen to decyl to decyloxy to native oxide, is expected (Figures 4.2.1-4.2.3). The trend is further confirmed with the correlation between SHG parameters and chemical shifts in Si 2*p* core level photoelectron spectra reported for the modified surfaces [4]. These chemical shifts have been shown [5] to vary almost linearly with the formal oxidation state of silicon near a Si/SiO_2 interface, so they provide a useful measure of the extent of

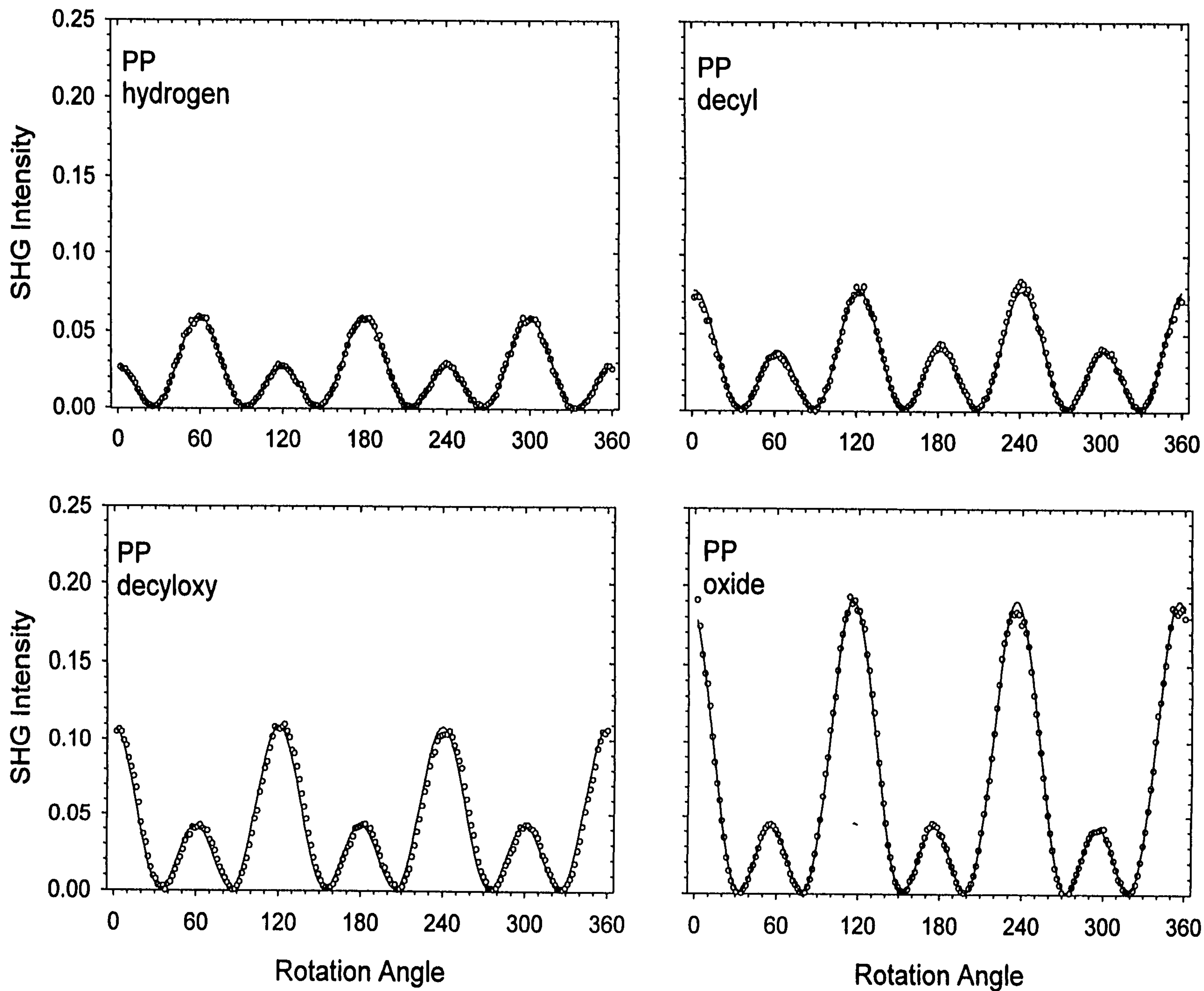

Figure 4.2.1 Comparison of chemically modified Si(111) surfaces at λ = 830 nm

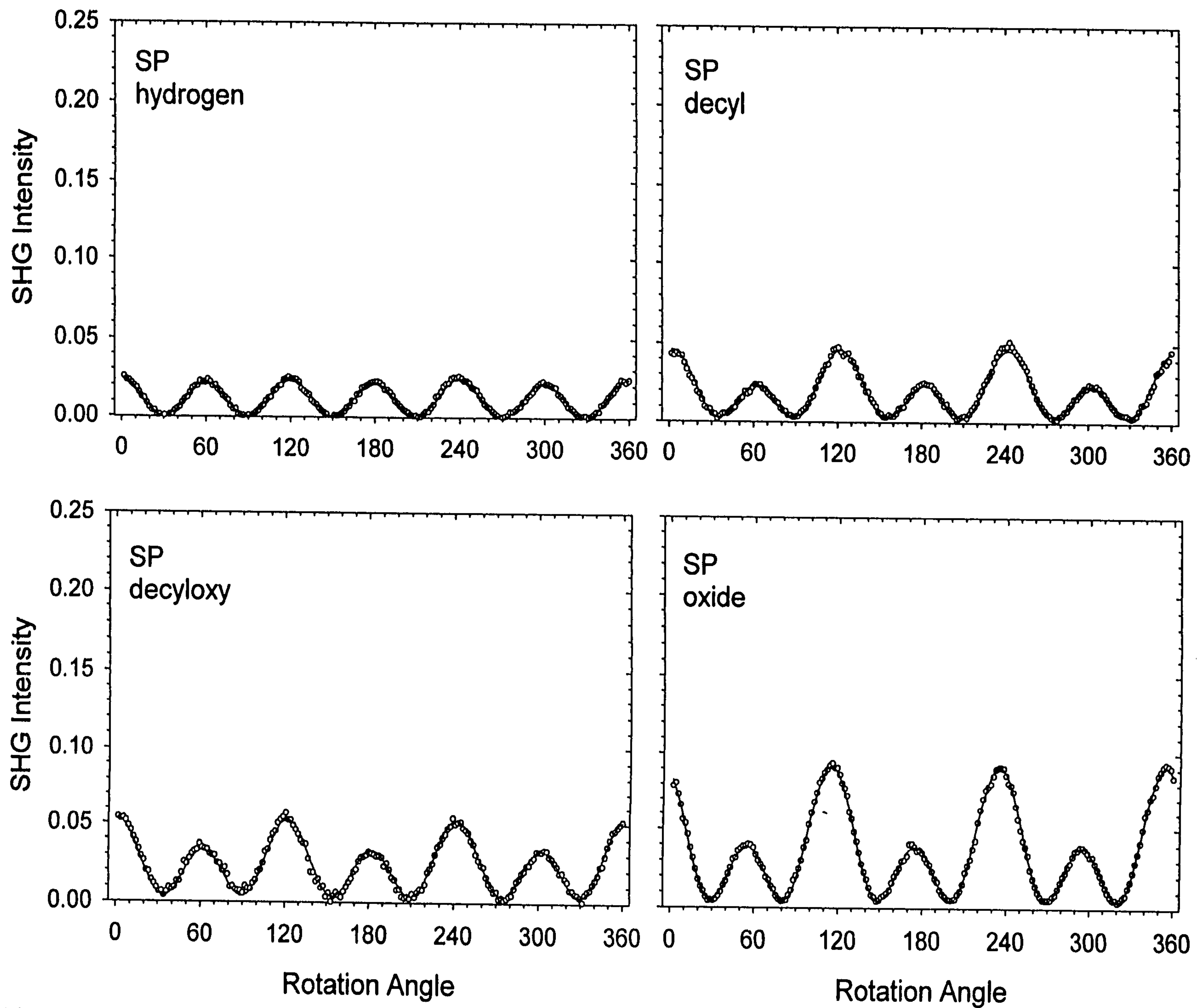

Figure 4.2.2 Comparison of chemically modified Si(111) surfaces at λ = 830 nm

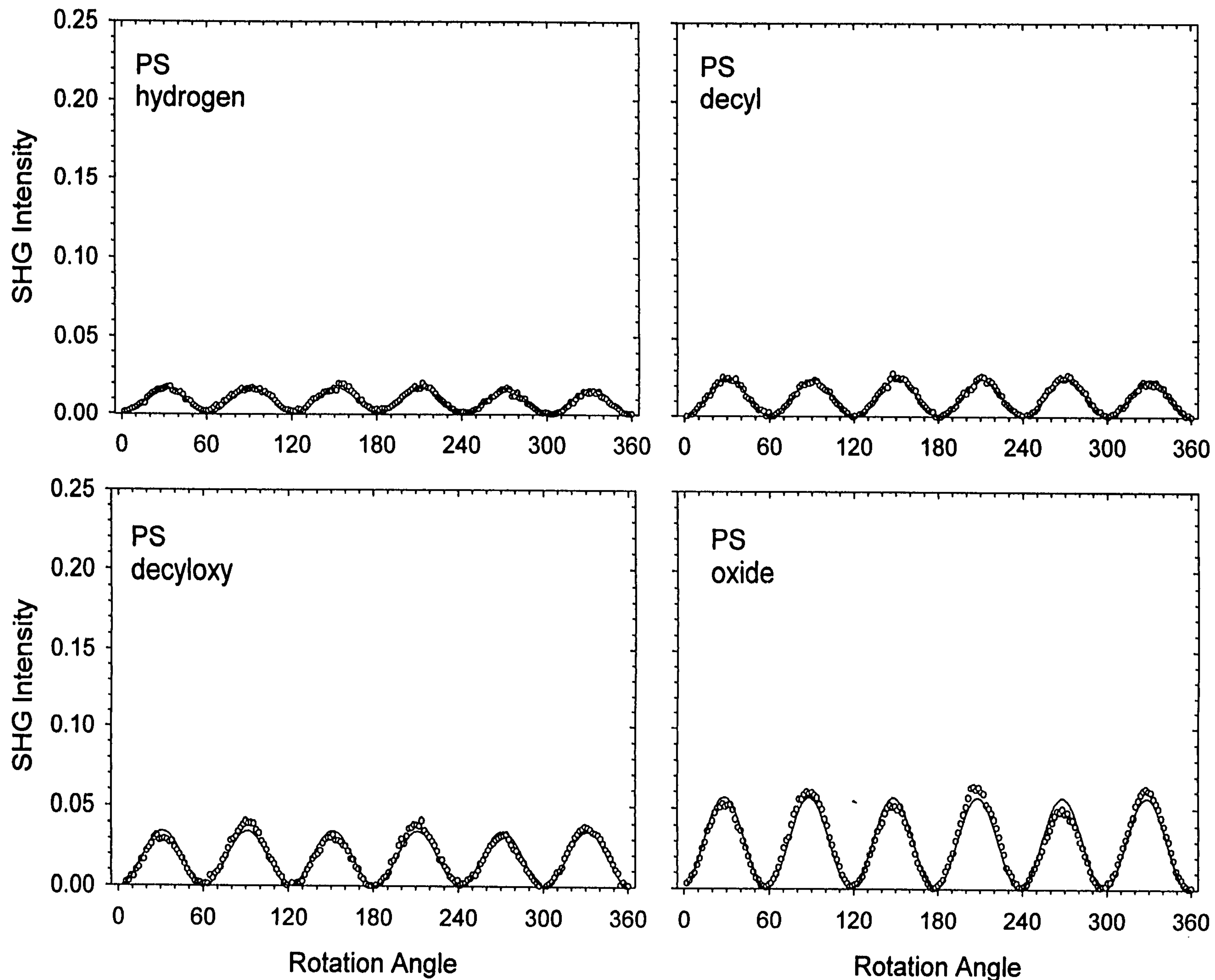

Figure 4.2.3 Comparison of chemically modified Si(111) surfaces at λ = 830 nm

polarization expected for the Si-Si back bonds. The low resistivity (1.16-3.04 Ωcm) of the Si(111) wafers used in all experiments ensured that the nonlinear optical response was independent of doping [6] and ruled out an electric field induced effect.

Since the electronegativity of the terminating species on a Si(111) surface determines the relative intensity of its rotational anisotropy and oxygen is the most electronegative of all substituents investigated, it is possible to monitor the increase of the SHG signal over time and correlate it with surface oxidation. Because the (p,s) polarization combination does not include an isotropic component, it is not ideal for this experiment. The differences between the (s,p) rotational anisotropy plots for the various surfaces (Figure 4.2.2) are not as striking as those for the (p,p) combination (Figure 4.2.1), especially for the Si(111)-H surface, so the latter polarization was selected as the best representation in all cases.

Surface stability studies in air were performed for two organic monolayers on Si(111): decyl and decyloxy. In the latter case, two thermal routes for preparation [4] were compared. Regardless of which route, using either decanal or decanol as a starting reagent, was employed to obtain a decyloxy terminated surface, the initial SHG signals exhibited no distinction, as shown in Figure 4.2.4. This is consistent with FTIR and X-ray photoelectron (XP) spectra reported by Wayner et al. [7], though they cite clear differences in chemical stability and topography for the two surfaces.

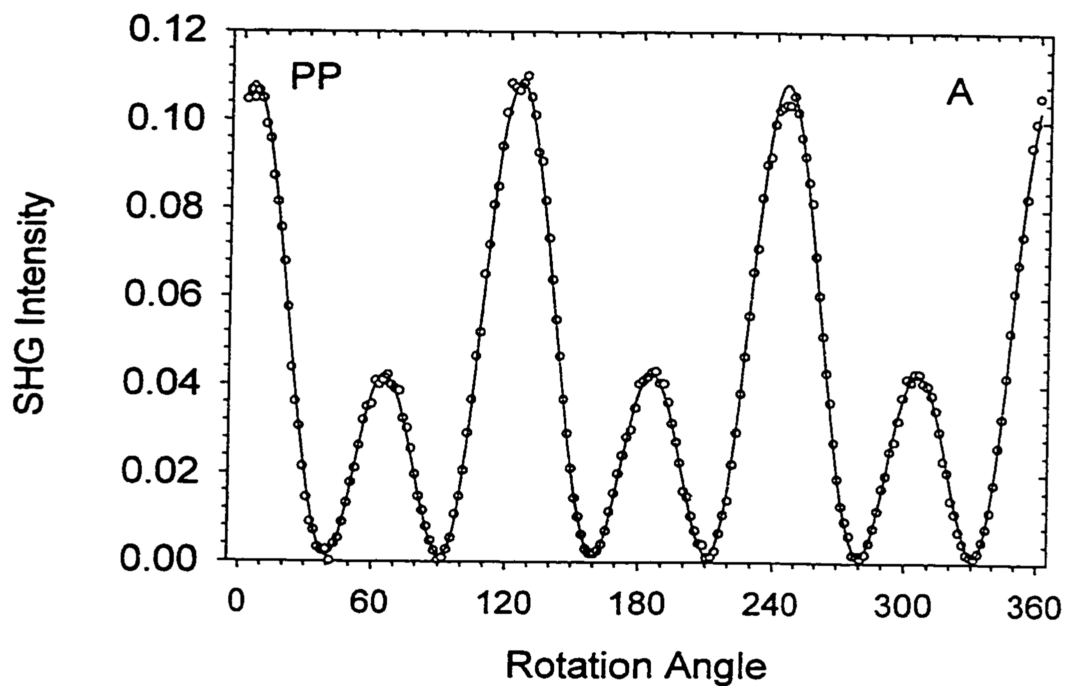

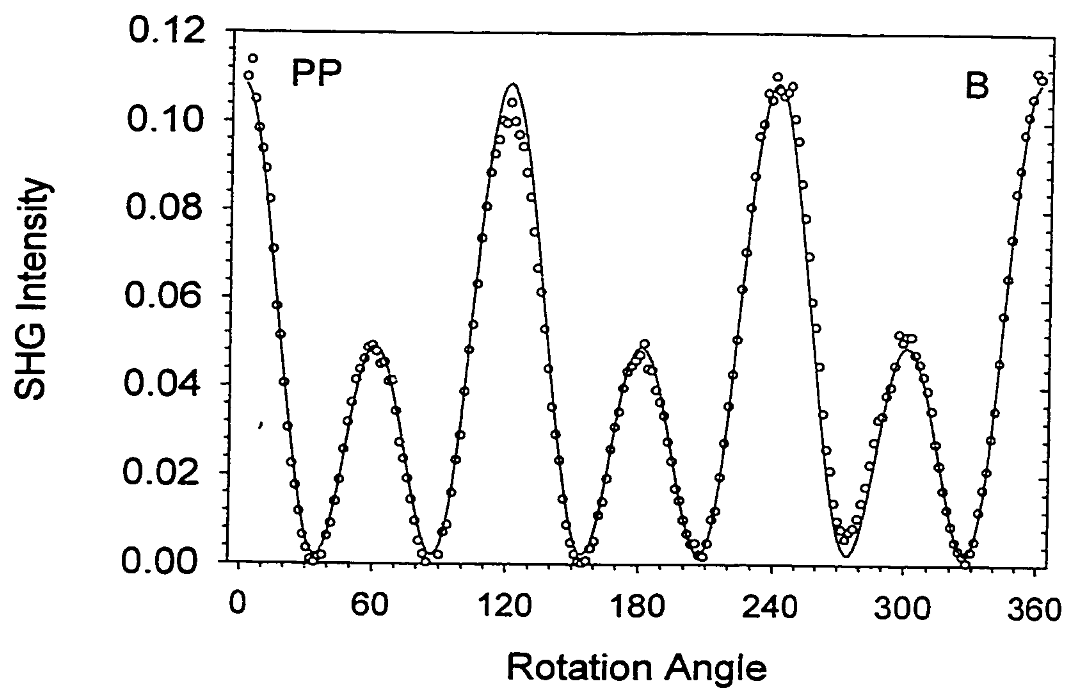

Figure 4.2.4 Comparison of decyloxy modified surface prepared by reaction with decanal (A) and decanol (B)

The Si(111)-H surface and the native oxide exhibit the most significant contrast in their respective signals. Due to the hydrogen terminated surface's affinity for reaction in air, this situation can be exploited by using SHG as a diagnostic tool to probe surface oxidation *in situ*. Two characteristics of the (p,p) rotational anisotropy plot for a Si(111)-H surface that are remarkably different from that of a native oxide sample are the angular positions of the large and small amplitude peaks and the relative signal intensity (Figure 4.2.1). The former difference is thought to be an indication of a nonlocal interaction associated with the gradient of the field [4] and, as described above, the latter is attributed to the difference in electronegativity of the terminating species.

Two methods of surface oxidation were investigated: exposure in ambient air, in the dark and with ultraviolet (UV) irradiation. As a control, to limit the effects of moisture and oxygen, a Si(111)-H sample was placed in a nitrogen purge and monitored over an extended period of time.

4.3. Stability of organic monolayers on Si(111)

A freshly prepared decyl terminated Si(111) surface was monitored over time to assess its stability in air. The rotational anisotropy plots, immediately after preparation and after three weeks in air, are compared in Figure 4.3.1. The values of α and γ remained the same, and several plots recorded during the course of the three week period confirmed that no change occurred, particularly not in the first 24 hours when significant oxidation was observed for the Si(111)-H surface. Wayner and co-workers [8] reported that this

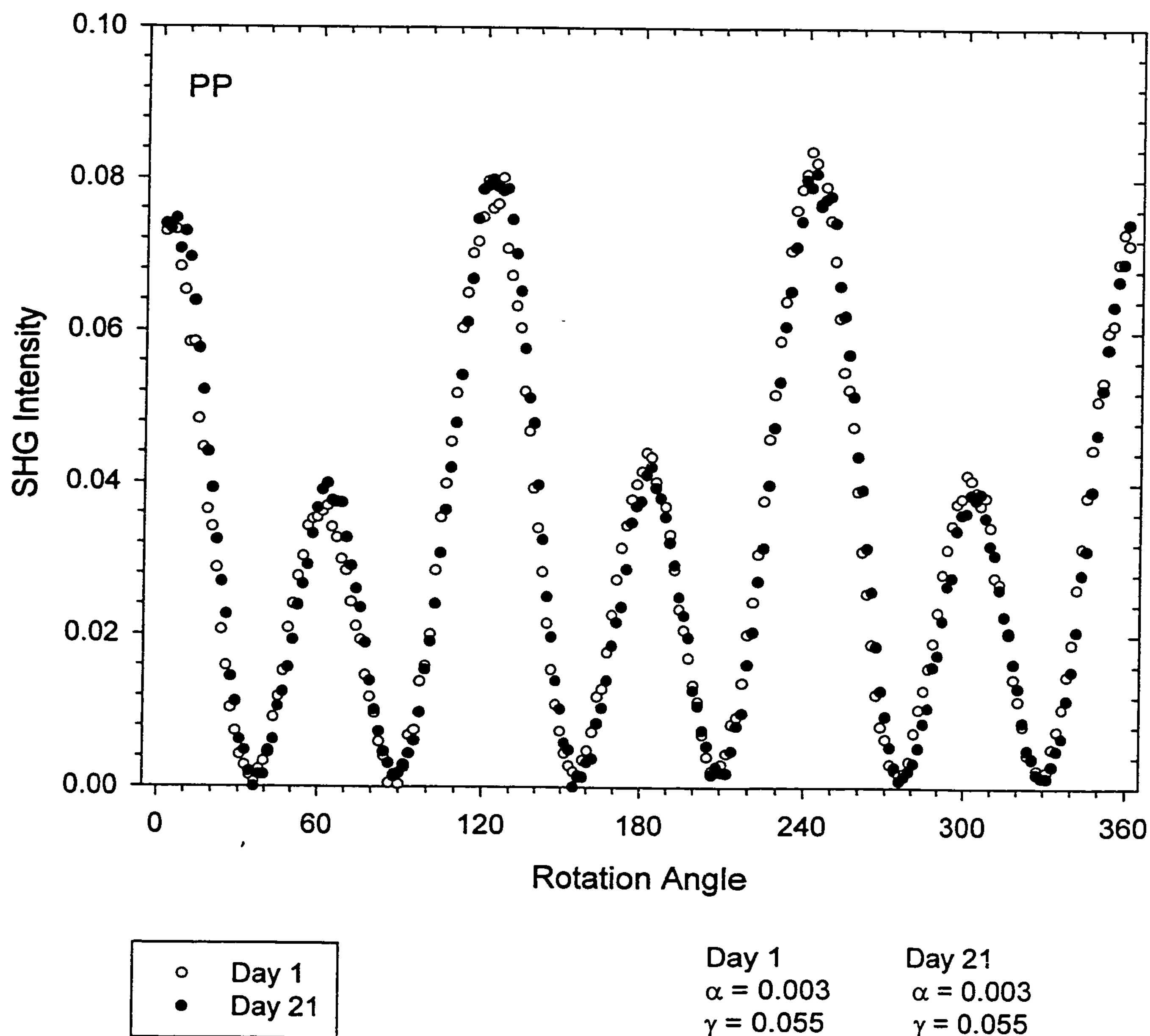

Figure 4.3.1 Comparison of SHG signal of decyl modified Si(111) surface over 21 days

modified surface was stable and can be stored for several weeks without any change in topographic or spectroscopic properties. In principle, the lack of surface oxidation and the appearance of the alkyl C-H stretch in the IR are also consistent with a physisorbed alkyl layer. In order to confirm the robust nature of the alkyl termination, the surface was subject to numerous harsh treatments: rinsing with trichloroethane, boiling in chloroform and in water for one hour each, immersion for 10 minutes in 40% NH_4F followed by 3 days in water and, finally, soaking in 2M KOH for 10 minutes [8]. Washing in organic solvent alone would be sufficient to remove physisorbed species [9]. With the exception of immersion in strong alkali, no significant decomposition of the alkyl monolayer was found, consistent with Chidsey's [10] earlier results.

A decyloxy modified surface obtained from the reaction with decanal showed a similar lack of oxidation over the initial 24-hour interval following preparation, as illustrated in Figure 4.3.2. This is in agreement with results reported by Wayner et al. [7], using XP spectra. They also found that AFM images of the surface after exposure to air were characterized by clear terraces and did not change in appearance following initial preparation. For the SHG study, after one week in air, an increase in γ was observed, suggesting there may be a certain degree of oxidation after an extended length of time. The difference in magnitude between the initial SHG signal for these organically modified surfaces, as compared to the native oxide, is a factor of two or less. For this reason, it would be advantageous to probe organic monolayers on silicon at wavelengths where resonance enhancement is observed [11] so that the contrast would be larger.

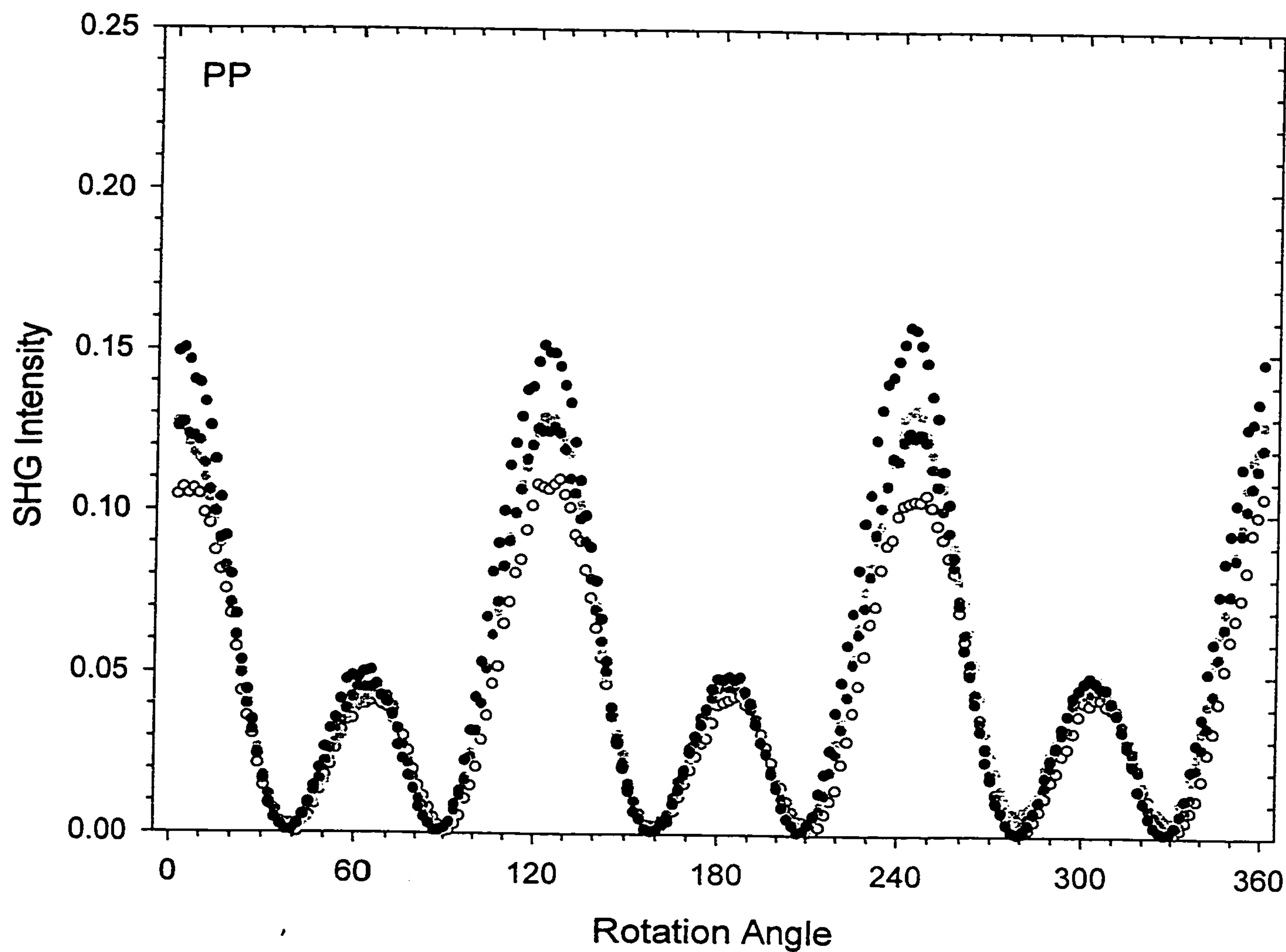

0 hours	3.5 hours	23 hours	172 hours
$\alpha = 0.005$	$\alpha = 0.009$	$\alpha = 0.007$	$\alpha = 0.007$
$\gamma = 0.070$	$\gamma = 0.078$	$\gamma = 0.079$	$\gamma = 0.093$

Figure 4.3.2 Comparison of SHG signal of decyloxy modified Si(111) surface, prepared by reaction with decanal, over 7 days

In Figure 4.3.3, the rotational anisotropy plots for a decyloxy modified surface obtained from the reaction with decanol indicate that the sample was significantly more reactive. This is in agreement with Wayner's [7] tests for surface robustness. Boiling in water, which etches any exposed silicon, reduced the hydrocarbon IR signal by half for the alcohol modified surface, while the signal dropped only marginally for the aldehyde modified surface. A reduction in adventitious etching by water or fluoride occurred when the reaction with decanol was carried out in the presence of chlorotrimethylsilane, a chemical scavenger, as shown by AFM images with clearer terraces and fewer etch pits [7]. By adopting this method of preparation, robust decyloxy surfaces can be obtained with either decanol or decanal as the starting reagent.

4.4. Oxidation of Si(111)-H

4.4.1. Hydrocarbon surface contamination of Si(111)-H

The structure of adsorbates on Si(100) is technologically relevant; however, there is no established technique to prepare an atomically flat Si(100) surface [9]. The ideally terminated Si(111)-H surface prepared by etching in aqueous NH_4F solution [12] presents a valuable model for the chemical reactivity of a well-defined silicon surface. It is generally accepted that the hydrogen termination acts as a passivation layer to protect the surface from contamination; however, the effect of organic contaminants has not been subject to a great deal of quantitative study. Uosaki and co-workers [9] undertook a method to monitor the surface contamination process on Si(111)-H. Using ATR-IR

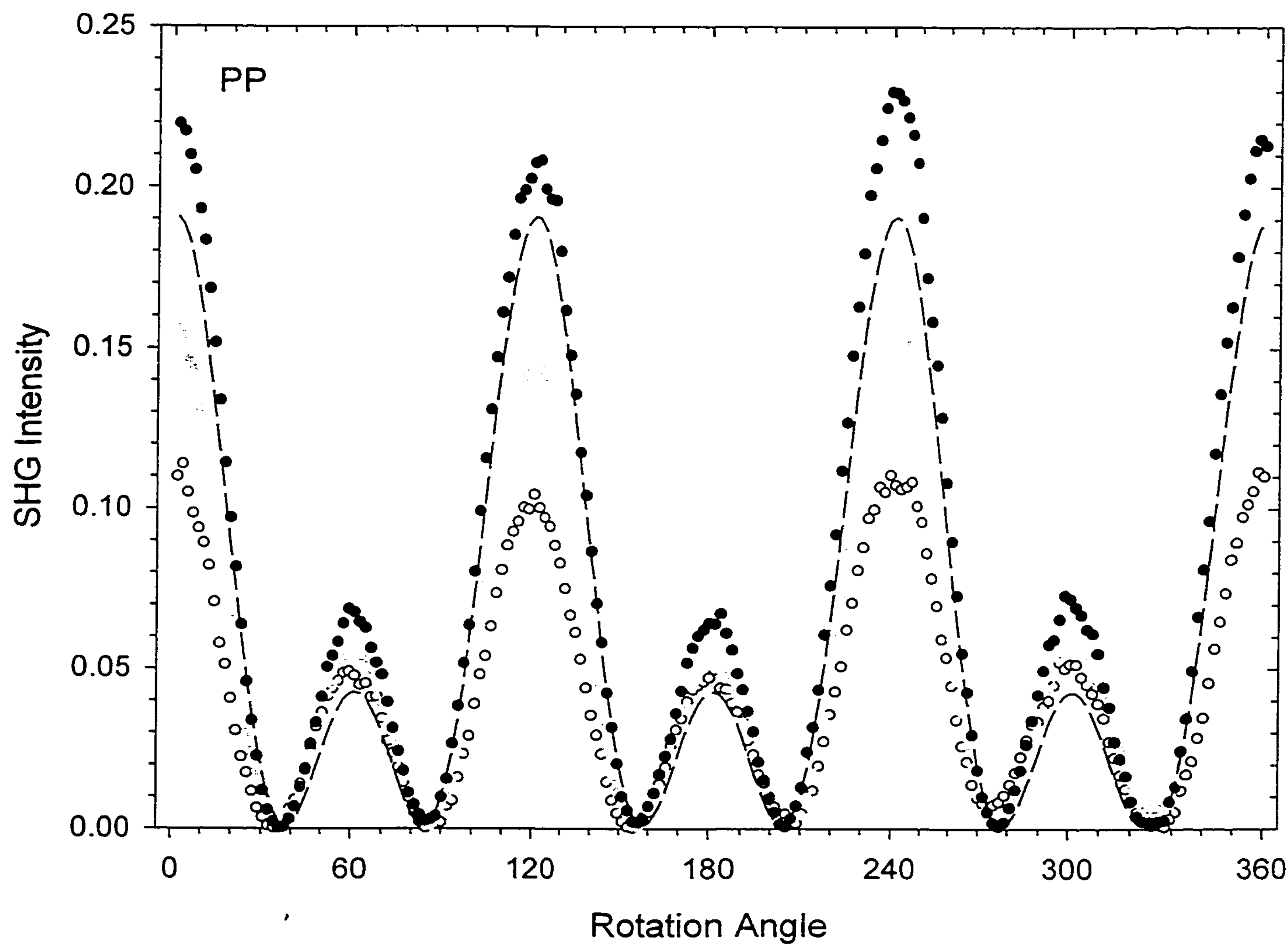

○ 0 hours
6 hours
● 22 hours
— — native oxide

0 hours	6 hours	22 hours	native oxide
$\alpha = 0.005$	$\alpha = 0.009$	$\alpha = 0.014$	$\alpha = 0.014$
$\gamma = 0.074$	$\gamma = 0.095$	$\gamma = 0.130$	$\gamma = 0.102$

Figure 4.3.3 Comparison of SHG signal of decyloxy modified Si(111) surface, prepared by reaction with decanol, over 1 day

spectroscopy, they measured the Si-H and C-H stretching bands as a function of exposure to dry air.

As exposure time increased, the peak height of the Si-H band decreased, in agreement with studies monitoring the oxidation of a Si(111)-H surface in air [13,14]. However, three peaks in the region of 3000-2800 cm^{-1} also appeared and were assigned to stretching modes of the methylene and methyl groups of hydrocarbon species adsorbed to the silicon surface. The etching process was eliminated as being the source of contamination since these peaks were not observed immediately after surface preparation. In the IR spectra taken following sonication of the sample in hexane, after five days of exposure to dry air, the sharp Si-H peak was recovered and the C-H bands were largely removed. This indicates that the Si-H band was not irreversibly decomposed and the hydrocarbon impurities on the surface were primarily physisorbed. Chidsey et al. [10] reported that the Si-H bands disappeared irreversibly after reaction of a Si(111)-H surface with 1-alkenes and suggested that the alkyl chains were chemically bound to the substrate through silicon-carbon bonds.

The conclusions drawn from the study of organic contaminants [9] on Si(111)-H also included the fact that the surface was hydrophobic and therefore promoted physisorption of organic species and that the position and width of the Si-H band was not affected, so likely the contaminants form islands on the surface. In contrast to other results [13], which included a peak at 2250 cm^{-1}, assigned to $SiH(O_3)$, oxidation of the surface was not observed. XPS measurements confirmed the absence of silicon oxide after five days

of exposure to dry air. Less than complete recovery of the Si-H peak after sonication in hexane was attributed to poor solubility of contaminants in hexane or a small amount of chemically bonded organic species on the surface.

Overall, hydrocarbon impurities reduce the Si-H vibration in the IR spectrum, which can lead to misinterpretation of the chemical reactivity of a surface. The response in a SHG experiment depends solely on chemically bonded species, making SHG a technique that can overcome the uncertainty that arises in IR studies, when assigning peaks to organic contaminant or oxidation species.

4.4.2. Nitrogen purge

A freshly prepared Si(111)-H sample was placed in the nitrogen purge box and rotational anisotropy plots were recorded immediately. As shown in Figure 4.4.1, measurements were taken one, two and eight days after preparation without appreciable change in the value of A or B. Even after 33 days, there was negligible change in the second-harmonic response of the surface. This experiment illustrates that, with a minimal presence of moisture and oxygen, surface oxidation is largely inhibited. This concurs with a study [15] where a Si(100)-H surface was placed in a dry nitrogen environment for one week. The growth of native oxide was limited to 1.9Å thickness, as measured by XPS combined with ellipsometry. In air, with a relative humidity of 42%, the film thickness was measured as 6.7Å.

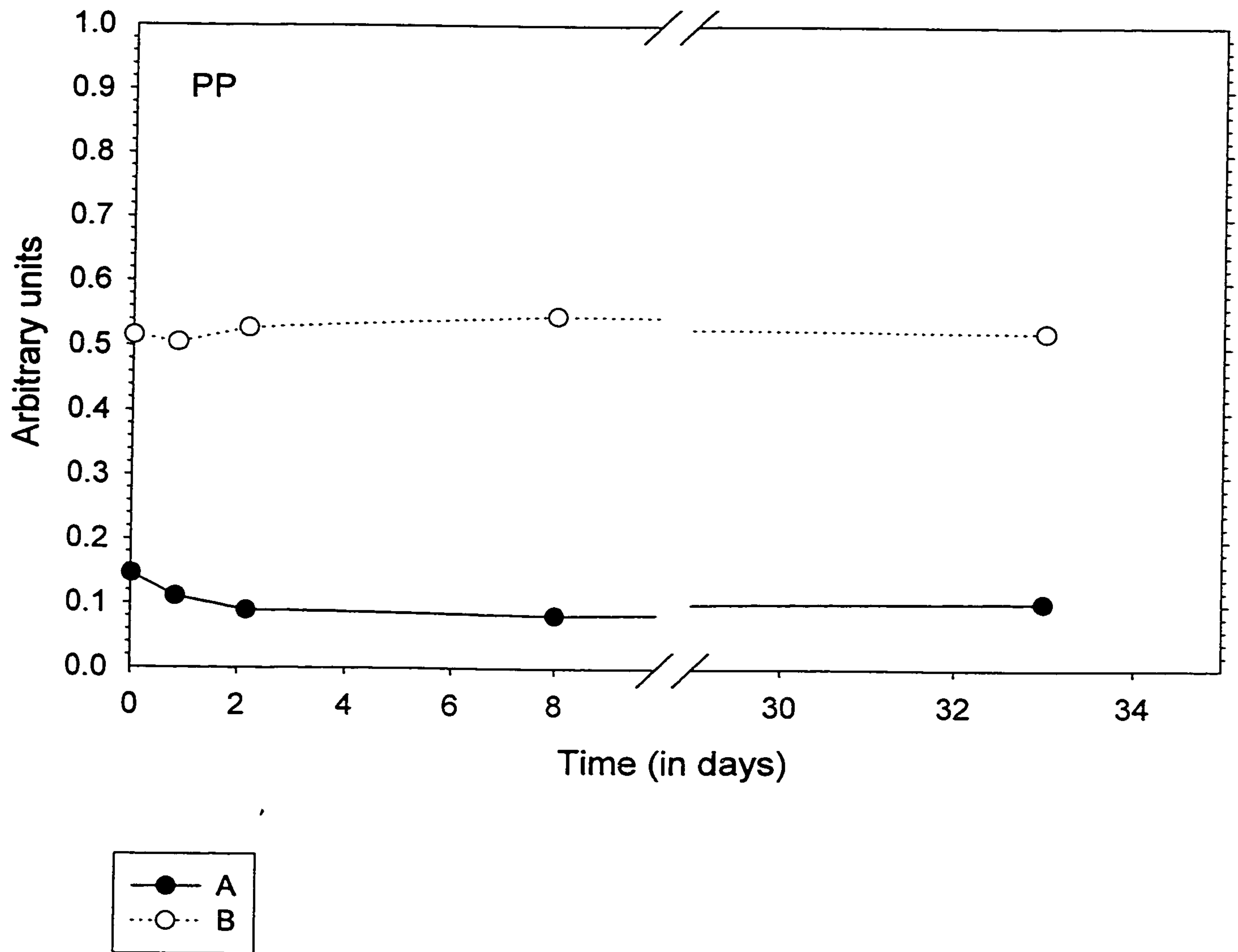

Figure 4.4.1 Monitoring of Si(111)-H sample in nitrogen purge

4.4.3. Exposure to ambient air in the dark

The evolution of surface oxidation, monitored for two separate Si(111)-H samples in ambient air in the dark, is shown in Figures 4.4.2 and 4.4.3. There are distinct transformations that can be seen both visually in the appearance of these SHG plots and graphically by plotting the isotropic and anisotropic components, A and B, of the signal and the ratio of one to the other, all versus exposure time (Figure 4.4.4). The most interesting observation for the sequential rotational anisotropy plots is the non-monotonic behavior of the signal. Consequently, in Figure 4.4.4, the values of A and B follow an alternating cycle of decreases and increases.

In Figure 4.4.2, the first eight hours of exposure to ambient air in the dark were chronicled with six plots. The signal underwent a gradual decrease during the initial five hours and then began increasing, with a phase change for the relative amplitude of alternate peaks apparent close to 8.5 hours after the sample was etched. In Figure 4.4.3, few time intervals were recorded during the early stages of oxidation. However, even after 20 hours, the phase change was only beginning to occur. Subsequent to this, after approximately three days in air, the signal intensity approached that of the native oxide. Further monitoring indicated that the signal decreased after several more days in air; and, even after prolonged storage in the order of weeks following preparation, the signal intensity was still substantially lower than that of the native oxide. The native oxide can be considered the 'final stage' for the surface oxidation of Si(111)-H; its rotational anisotropy plot is shown as a dashed line in Figures 4.4.2 and 4.4.3. The later stages of

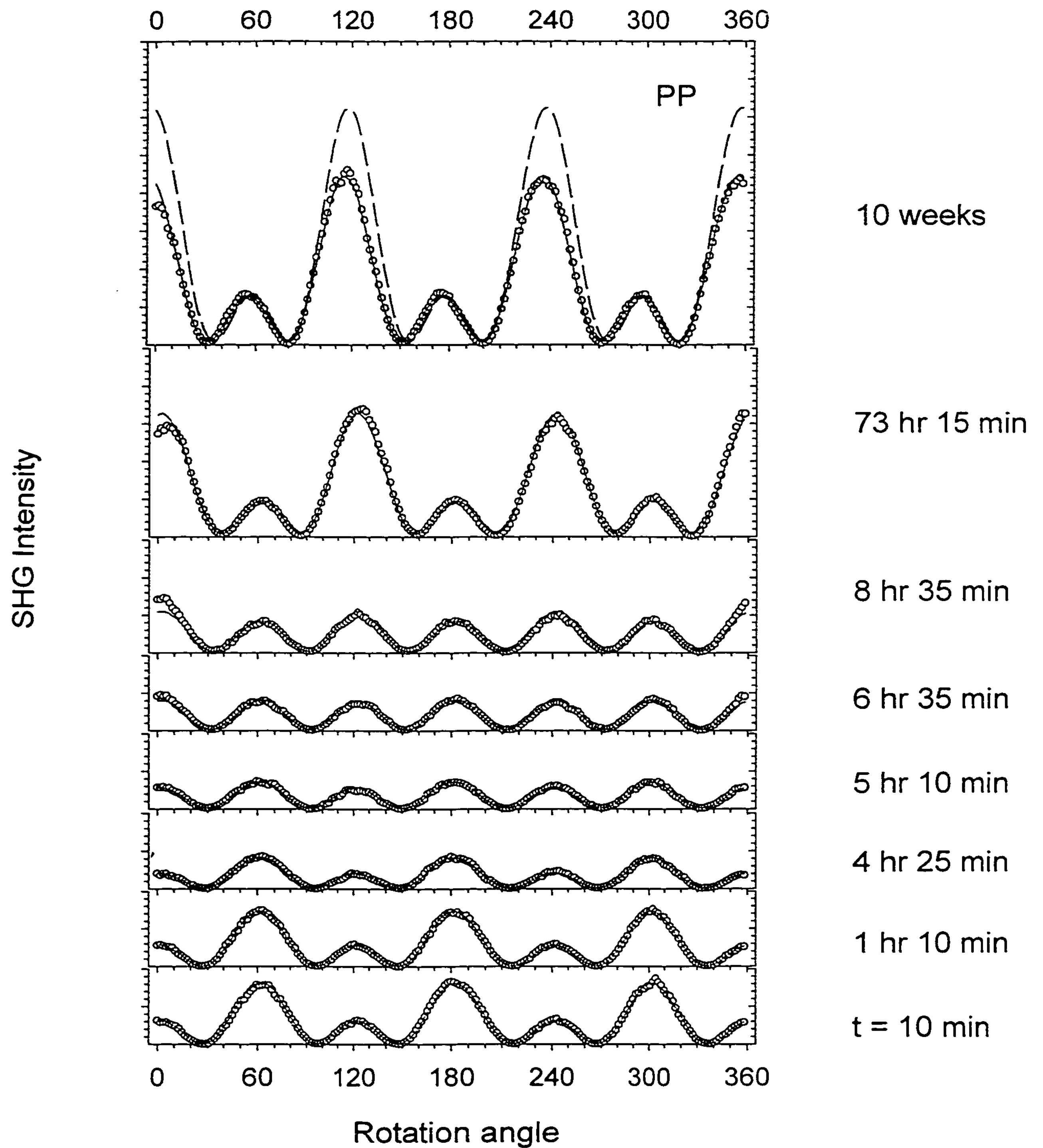

Figure 4.4.2 Evolution of Si(111)-H surface oxidation over time in ambient air in the dark. Dashed line in top plot is native oxide SHG signal

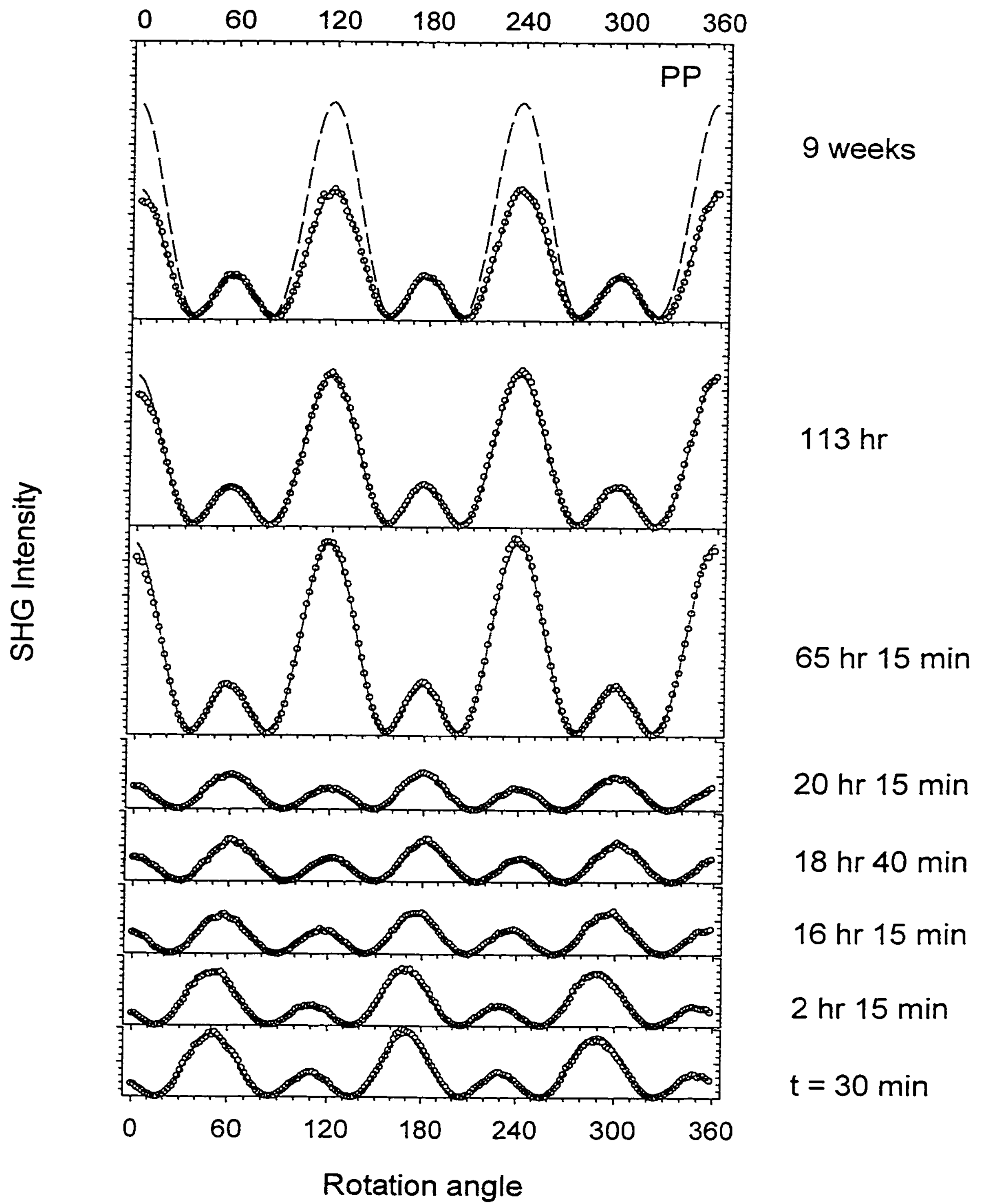

Figure 4.4.3 Evolution of Si(111)-H surface oxidation over time in ambient air in the dark. Dashed line in top plot is native oxide SHG signal

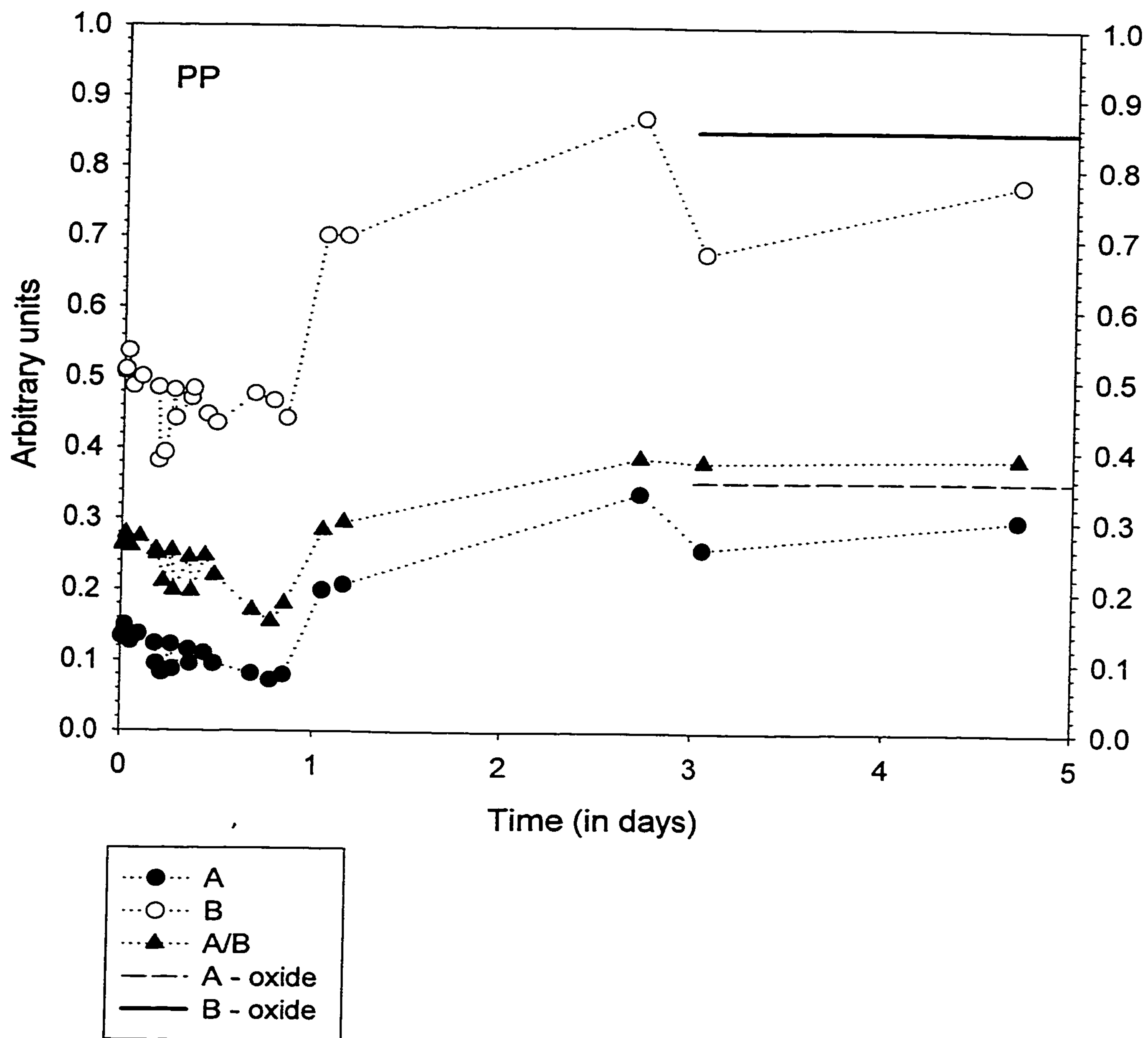

Figure 4.4.4 Evolution of SHG parameters for Si(111)-H surface oxidation over time in ambient air in the dark

oxidation captured in Figure 4.4.2 show that the signal's increase is less pronounced between 8.5 and 73.25 hours than between 20.25 and 65.25 hours in Figure 4.4.3. However, long-term exposure in the two cases (9 or 10 weeks) seemed to produce nearly identical rotational anisotropy plots. Other Si(111)-H samples prepared and monitored over time exhibited similar discrepancies, but they still demonstrated that the surface oxidation is non-monotonic as discussed above.

Evidently, there is a reasonable amount of sample-to-sample variation in the rate at which the signal intensity evolves. This can be attributed to factors such as the amount of residual NH_4F on the surface and relative humidity. For all experiments described here, there was no rinsing with water done after the sample was removed from the etching solution. It has been suggested that adding this step can reduce the level of contamination of the sample [16]. Several studies [13,14], performed in low humidity environments, support the fact that the amount of moisture present is critical in determining the rate and extent of surface oxidation.

The SHG parameters for Si(111)-H oxidation, shown in Figure 4.4.4, were extracted from the rotational anisotropy plots of Figures 4.4.2 and 4.4.3 and additional samples (not shown). The isotropic component has contributions from the Si-Si bonds which are parallel to the surface normal, while the anisotropic component is influenced by the threefold symmetry of Si-Si back bonds in the substrate. The perspective view of two bilayers of a Si(111)-H surface in Figure 1.3.2b (page 7) clearly shows these bonds. The

values of A and B for the native oxide signal are also plotted, as a line to guide the eye, for comparison.

For the Si(111)-H surface, B is slightly more than three times larger than A, but the non-monotonic transformation of both components was observable over the course of time. The initial downward trend for the values of A and B persisted for the first 24 hours. The subsequent abrupt increase, most noticeable in the anisotropic component, was coincident with a sharp drop in phase angle. Over the next few days of exposure, the signal continued to steadily increase, followed by a moderate decrease. The values of A and B recorded nine or ten weeks later do not differ significantly (not shown in Figure 4.4.4). This constancy in the parameters over long periods of exposure can be supported by photoelectron spectra obtained by Miura et al. [14], indicating a saturation thickness for the growth of native oxide. Between 4 and 42 days after initial preparation, with a relative humidity of 40%, the Si(111)-H surface in their experiments maintained a native oxide layer approximately 6Å thick.

A simple model suggests that A and B are proportional to the number of Si-Si bonds present at the surface. Therefore, in this model, a Si-Si bond represents a one and a Si-O bond represents a zero. With the simultaneous oxidation of all three Si-Si back bonds for a given surface silicon atom, as suggested by Niwano [13], the number of Si-Si bonds is rapidly reduced and the signal drops in intensity. This phenomenon is represented in Figure 1.6.1 (page 18) and labeled *intrabilayer insertion*. When fully oxidized, the top bilayer becomes effectively transparent, as a second-harmonic signal is no longer

generated from this surface. *Interbilayer insertion* of atomic oxygen in the silicon substrate allows polarization of the Si-Si back bonds of the second bilayer and these begin to contribute to the SHG response, increasing the signal intensity. The next Si-Si bonds available for attack are the back bonds of the second bilayer. Intrabilayer insertion occurs again, and, accordingly, the response will tend to decrease. The degree to which each step (intra- or interbilayer insertion) proliferates before the next step begins to occur is not known. As detailed in the Introduction section, a layer-by-layer mechanism is favored.

Interpretation of the non-monotonic behavior, based on this simple model, suggests that the decrease over the first day after preparation can be attributed to Si-Si back bond oxidation. If the Si-H bonds were attacked first, this would lead to an increase in signal intensity, as a Si-OH bond is more electronegative than a Si-H bond, and the Si-Si back bonds of the topmost bilayer would be more strongly polarized. The absence of this occurrence is in agreement with Niwano's [13] results, where the $SiH(O_3)$ peak persisted for long periods of time. Following the extensive intrabilayer insertion, the signal undergoes a rapid increase in intensity. If the intrabilayer insertion happened concurrently with the interbilayer insertion, which is the most rational cause for the parameters getting larger, the slope would not be expected to be very steep, particularly for the A/B ratio, because the contributions from one process would cancel out the other. This leads to a mechanism where interbilayer insertion must predominate, correlated with a significant change in A. This phenomenon polarizes the Si-Si back bonds of the second bilayer, once the first bilayer is almost entirely oxidized and no longer contributing to the SHG signal.

The subsequent reduction in the strong contribution to the SHG response by interbilayer oxygens can be rationalized by intrabilayer insertion occurring once again. After several days of exposure, the oxygen species' rate of penetration into the substrate is likely impeded, hence the gradual nature of the signal intensity's decrease and the plateau evident in the A/B ratio. The leveling off of the SHG response over much longer periods of time correlates well with the decline in accessible and favored sites for oxygen insertion close to the surface, *i.e.* those that do not cause a large degree of strain in the crystal structure [17].

4.5. Photo-oxidation of Si(111)-H

4.5.1. 350-nm broadband irradiation in ambient air

A freshly prepared Si(111)-H surface was irradiated with 350-nm broadband UV light from a mercury (Hg) pen lamp, with an irradiance of ~ 0.4 mW/cm^2. After 15 minutes of continuous irradiation, very little change was observed in the susceptibilities A and B. An additional 45 minutes of irradiation did not alter the signal significantly enough to detect any difference between this sample and one exposed to air without irradiation for one hour, as shown in Figure 4.5.1. Chidsey and co-workers [18] reported a ten percent decrease in the ATR-IR peak for Si-H, following 350-nm illumination in air of a Si(111)-H surface, with an irradiance of ~8.9 mW/cm^2 for 54 minutes. Attenuation of the broadband 350-nm light, with a microscope slide to exclude wavelengths shorter than 300 nm, did not affect the IR spectrum. This confirmed that the 350-nm light was

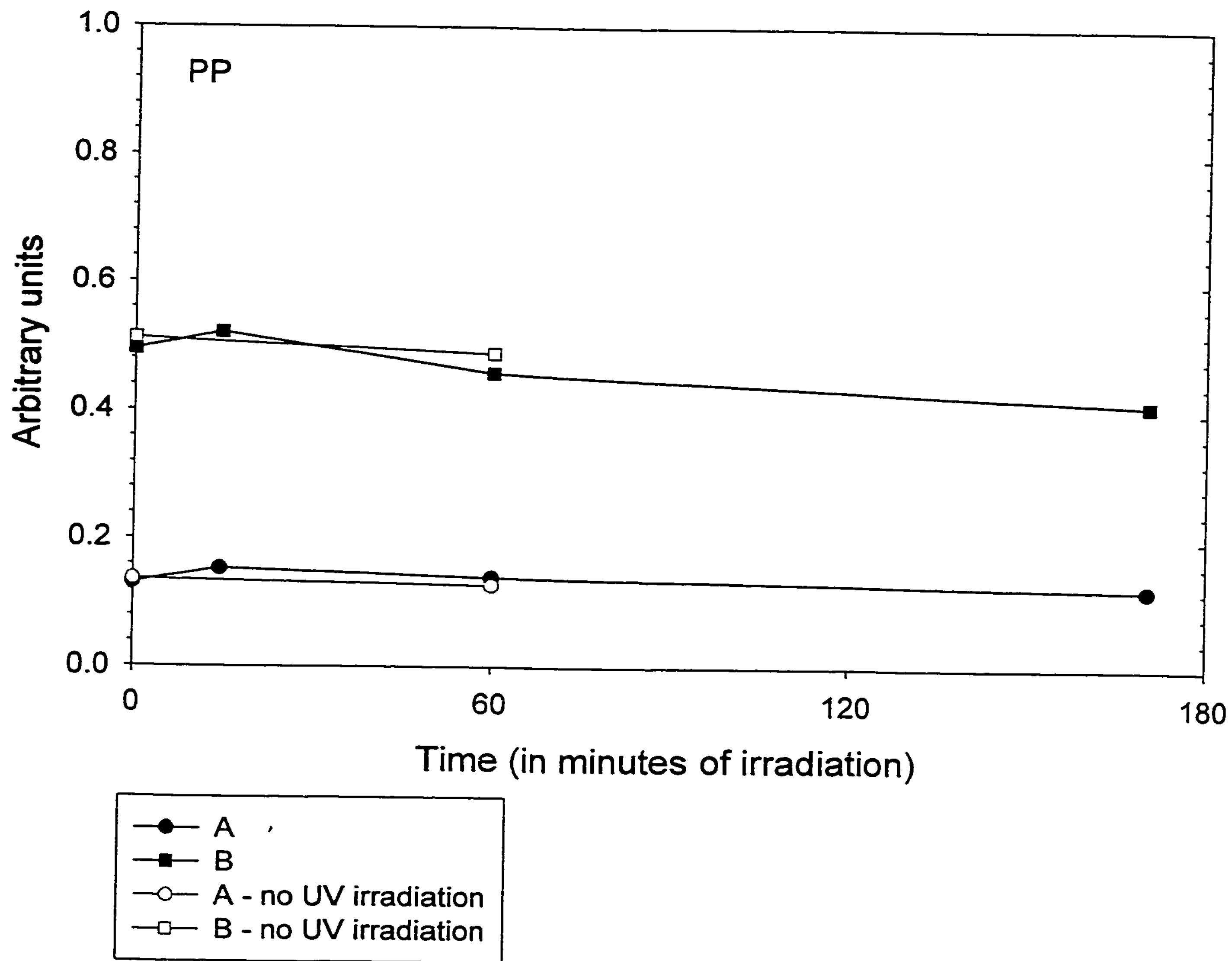

Figure 4.5.1 Comparison of the evolution of Si(111)-H surface oxidation over time, with and without broadband 350-nm irradiation, in ambient air

responsible for the photo-oxidation, not trace amounts of the 254-nm wavelength that might be present. Ellipsometry indicated that a film no thicker than 1Å was formed. With exposure to 450-nm broadband light, no detectable amount of oxidation was observed, so their results suggest that 350 nm is the threshold wavelength for activation of the Si(111)-H reaction with oxygen. In our case, after 170 minutes of 350-nm broadband irradiation, only 14% as much energy was delivered to the surface, so an absence of change in the signal is not unexpected.

4.5.2. 254-nm irradiation in ambient air

For 254-nm irradiation, with the Hg lamp placed at the same distance from the sample as for the 350-nm broadband irradiation described above, the irradiance was ~7.4 mW/cm^2. A freshly prepared Si(111)-H surface was exposed for two minutes to this irradiation and the susceptibilities were larger than those of the native oxide. Another freshly prepared Si(111)-H surface was subject to 20 minutes of exposure and similar results were obtained, suggesting that there may be a limit to the degree of photo-oxidation possible with UV light.

After 30 minutes of 254-nm exposure with an irradiance of ~16 mW/cm^2 in Chidsey's work [18], the Si-H peak decreased to 14% of its original value. This irradiation time delivered the same amount of energy to the surface as in their 350-nm broadband illumination experiment. XPS data correlated the oxide formation, as a strong oxygen 1*s* signal was observed and a chemically shifted Si 2*p* signal at ~103 eV indicated the presence of SiO_2. Ellipsometry measurements indicated that the film was 8Å thick. To

duplicate the energy delivered to the surface, 65 minutes of exposure would be required with our Hg lamp. After two minutes of exposure to 254-nm light, they observed a reduction to 83% of the original signal. Directly comparing the degree to which the Si(111)-H surface is oxidized in Chidsey's ATR-IR experiments versus our SHG experiments is not trivial. As previously discussed, IR spectroscopy has the inherent disadvantage that physisorbed species can falsely suggest that hydrogen termination has been lost [9], when this is not the case. A thorough set of experiments where both measurements would be performed on each sample would help make this comparison possible.

4.5.3. Continuous monitoring of signal during 254-nm irradiation

For the studies monitoring the Si(111)-H surface oxidation over time in ambient air in the dark, rotational anisotropy plots were recorded at incremental points hours, days and even weeks after initial preparation. From these plots, the isotropic and anisotropic components of the SHG signal were extracted. UV light exposure accelerates the reaction of the Si(111)-H surface with oxidative species, permitting the oxidation to occur over a much shorter time scale. By virtue of this, the changes observed for the isotropic and anisotropic components of the SHG signal can be monitored continuously. Each component may be isolated by rotating the sample so that $\phi = 30°$, where ϕ is defined as the angle between the plane of incidence and a <2-1-1> direction on the (111) surface. With the (p,p) polarization combination, the rotational anisotropy equation collapses from

$$R_{pp} = \alpha_{pp} + \gamma_{pp} \cos^2(3\phi) + \beta_{pp} \cos(3\phi) \qquad 4.5.1$$

to give only the isotropic component, α_{pp}. Similarly, with the (p,s) polarization combination,

$$R_{ps} = \gamma \sin^2(3\phi) \qquad 4.5.2$$

collapses to give only the anisotropic component, γ_{ps}.

The purpose of this experiment is not only to enable monitoring of the two components of the SHG signal separately, but also to allow interesting changes to be pinpointed to a specific length of UV exposure time, provided that surface oxidation behavior is quite reproducible from sample to sample. Given this, incremental rotational anisotropy plots could be recorded to present a complementary visual representation of the signal's evolution over time and to permit qualitative comparison to the plots obtained for surface oxidation in ambient air in the dark. One important contrast between incremental and continuous monitoring is the amount of the time that the laser beam is incident on the sample. Considerations of fluence on the sample and any consequent damage to the surface had to be addressed. This was achieved by continuous monitoring of the signal without exposing the sample to UV irradiation. A Si(111)-H sample, which had been exposed to air for three weeks, and one that was freshly prepared, were examined and, as Figures 4.5.2a and b attest, there was no detectable change in the signal for either case. This confirms that the fluence at the surface is insufficient to damage the sample. In the case of the freshly prepared sample, the laser did not induce oxidation such that it was observable in the anisotropic component of the signal, which changes much more significantly during oxidation than the isotropic component.

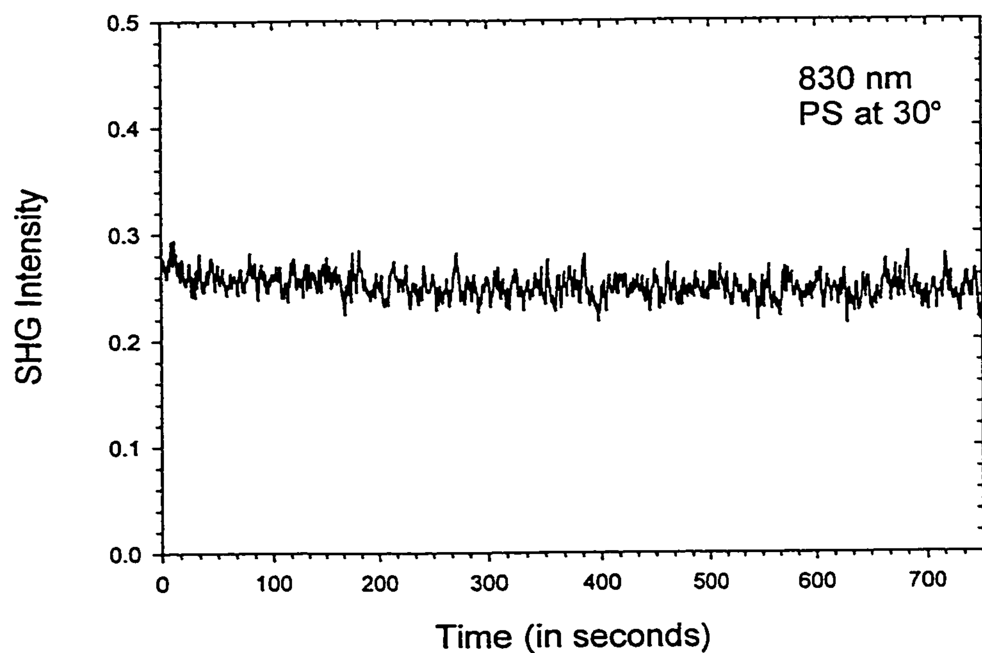

Figure 4.5.2a Si(111)-H surface monitored 19 days after fresh preparation

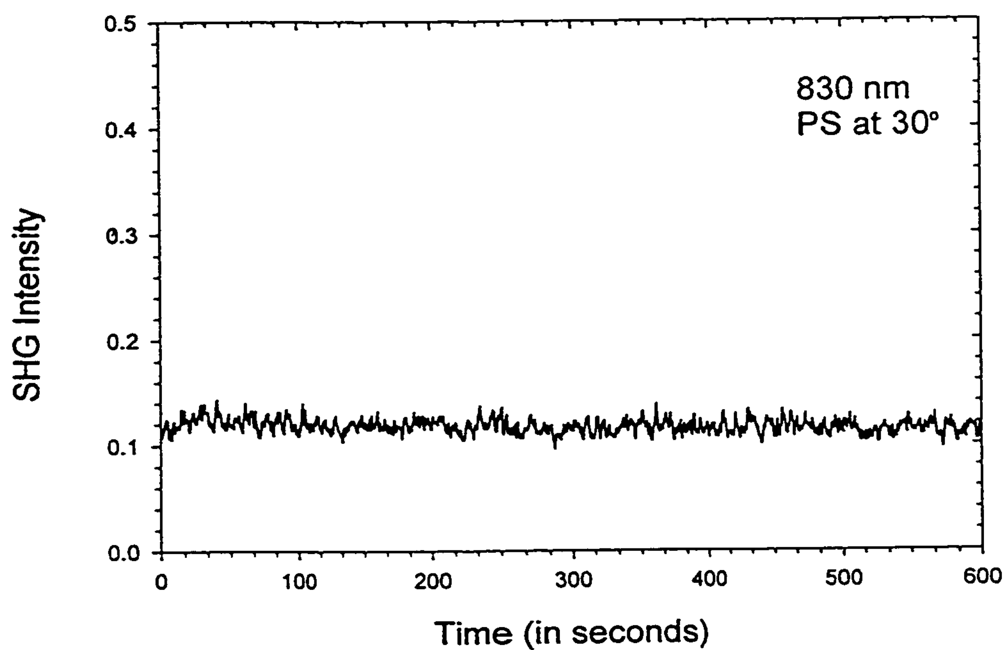

Figure 4.5.2b Si(111)-H surface monitored 30 minutes after fresh preparation

The first experiments with continuous monitoring were performed using the (p,p) polarization combination; however, due to the small size of the isotropic signal, it was difficult to accurately orient the sample at 30°. This resulted in recording a signal that was not purely isotropic and, since this component is subject only to a shallow decrease and then a fairly gradual increase over time during surface oxidation, pinpointing times at which the overall SHG signal underwent noticeable change presented a real challenge. The anisotropic component is a better component to use for tracking the progress of surface oxidation for hydrogen terminated silicon.

The most striking feature of the continuous monitoring for the (p,s) polarization combination at 30° is the non-monotonic behavior of the signal. The appearance of this decrease-increase-decrease-constant sequence for the signal intensity is very similar to that observed for surface oxidation in ambient air in the dark. XPS measurements [19] on a sample after irradiation for 25 minutes revealed that the native oxide thickness was 4Å. An as-received native oxide silicon wafer was shown to have an 8Å thick layer. A Si(111)-H surface oxidized in ambient air for eight hours was measured using ellipsometry. The film thickness was ~9 Å [20]; however, oxide film thicknesses are overestimated by ellipsometry [21].

An attempt to modify the photo-oxidized wafer by four different alkylation routes: photo-initiated, Lewis acid hydrosilylation and platinum catalyzed reactions with decene and thermal reaction with decylmagnesium bromide, yielded a hydrophilic surface in all cases [22], indicating that alkyl termination did not occur. This suggests that the photo-oxidized

Si(111)-H is no longer hydrogen terminated or the $SiH(O_3)$ species present do not react identically as compared with the freshly etched surface, possibly due to the strong polarization of the Si-H bond by the oxygens inserted in the back bonds.

Octadecyltrichlorosilane (OTS) requires a hydroxylated surface as a substrate for self-assembled monolayer formation [23]; therefore, it is unreactive toward hydrogen termination. The result obtained for the reaction of the photo-oxidized surface with OTS suggests that silanol (Si-OH) groups terminate the surface. Ellipsometry measurements indicated the presence of a 45Å layer [22], which correlates well with the expected thickness for a monolayer of octadecyl chains bound perpendicular to the substrate by formation of Si-O-Si bonds at the surface [23].

4.5.4. Incremental monitoring of signal during 254-nm irradiation

The initial experiment for UV irradiation of a Si(111)-H surface was performed before any continuous monitoring studies had been undertaken. Based on trials, summarized in Section 4.5.2, to determine an appropriate length of exposure and distance from the sample for the Hg lamp, the Si(111)-H sample was irradiated in two minute increments for a total of eight minutes with the lamp positioned 17.5 cm away from the sample, producing an irradiance of ~0.15 mW/cm^2 at the surface. The rotational anisotropy plots were recorded after each interval and again, 3 days afterwards, as illustrated in Figure 4.5.3.

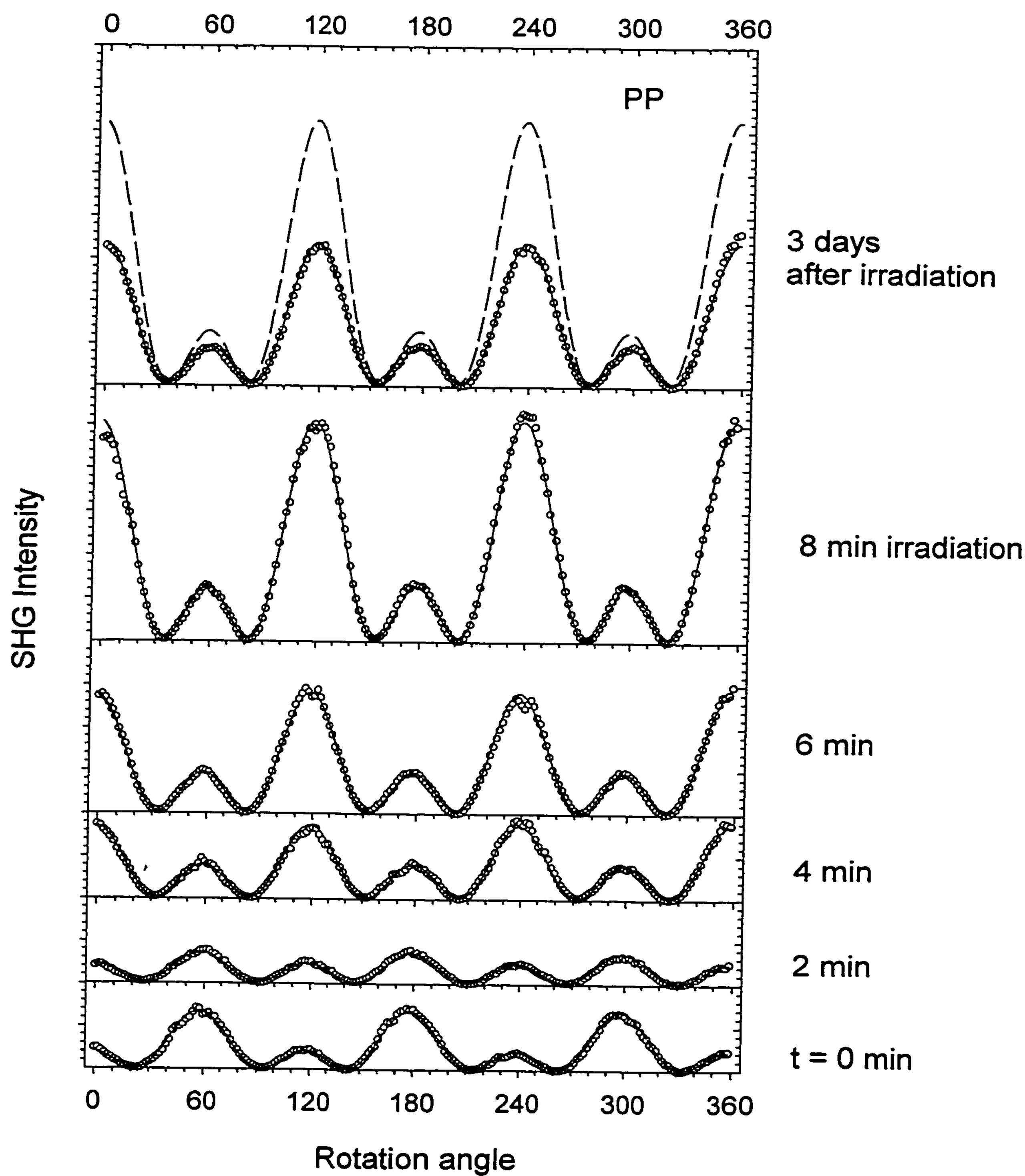

Figure 4.5.3 Evolution of Si(111)-H surface oxidation over time as a function of UV irradiation in ambient air. Dashed line in top plot is native oxide SHG signal

The advantage of incremental monitoring over continuous monitoring is the ability to track both the isotropic and anisotropic components of the signal during the surface oxidation. Using the continuous monitoring studies, optimum times for taking rotational anisotropy plots during the UV irradiation were determined. As shown in Figure 4.5.4, after 2.5 minutes of UV exposure for a freshly prepared Si(111)-H sample, the SHG signal decreased. After 5 minutes, the relative phase of the large and small peaks had changed and a steady increase in the signal was observed thereafter. After 25 minutes, the signal was larger than that of the native oxide, as predicted from the continuous monitoring studies. It is evident that, even after as little as two hours following UV irradiation, the signal dropped significantly and, after 24 hours (plot not shown), there was a further decrease to an intensity comparable to that of a rotational anisotropy plot recorded three days after irradiation, for a different Si(111)-H surface, shown in Figure 4.5.3. This latter sample was only irradiated for eight minutes, but it appears that a similar degree of oxidation was obtained over the long term, despite the shorter exposure time in this second case.

Figure 4.5.5 illustrates the conjunction of the B parameters from incremental and continuous monitoring studies and indicates that despite sample-to-sample variability, the agreement is excellent and the trend for the change in the anisotropic component is identical. The value of B for the native oxide is shown for comparison. It draws attention to the match of B immediately after the 25 minutes of UV irradiation and then the subsequent decrease that occurs over the next 24 hours of exposure in the dark.

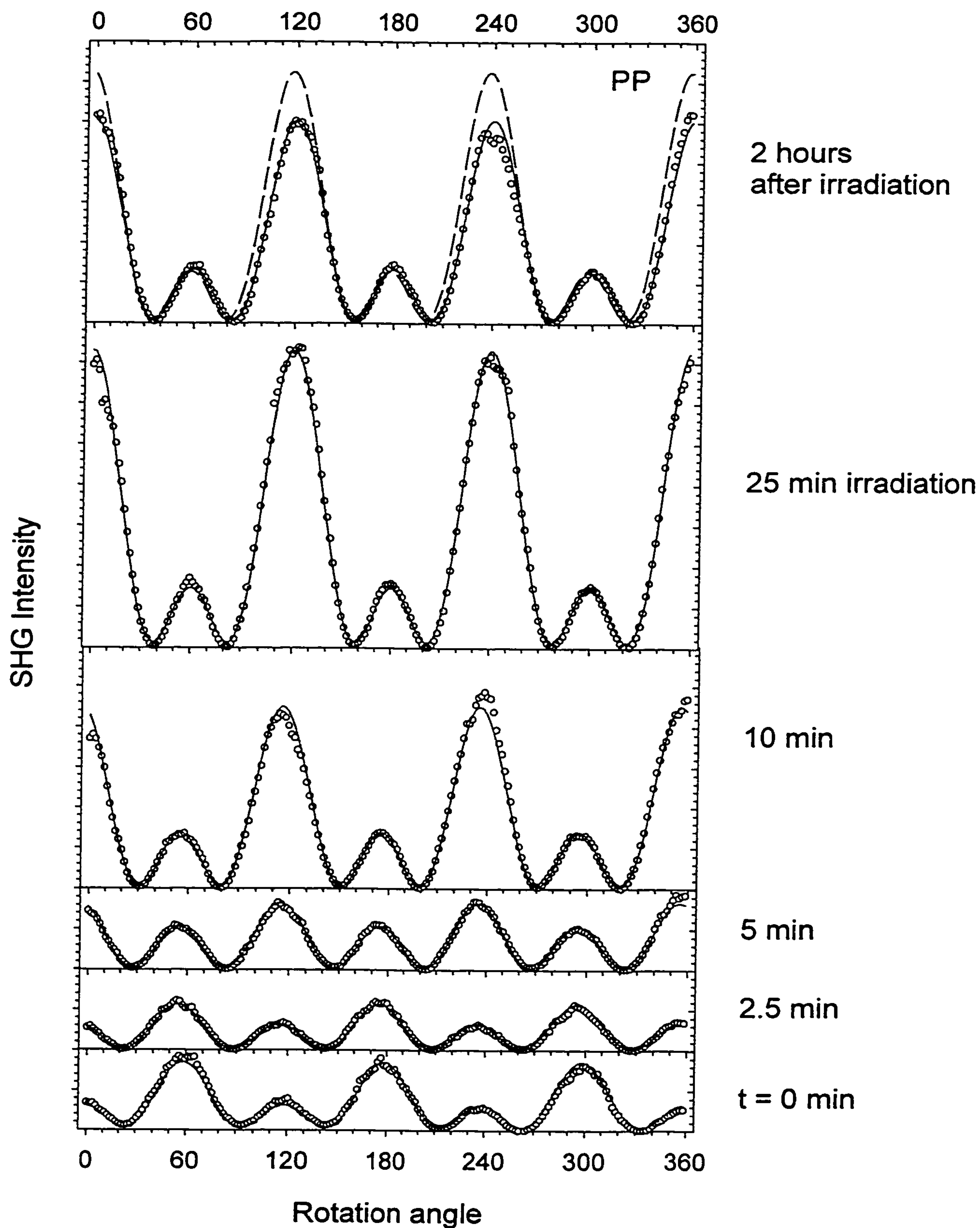

Figure 4.5.4 Evolution of Si(111)-H surface oxidation over time as a function of UV irradiation in ambient air. Dashed line in top plot is native oxide SHG signal

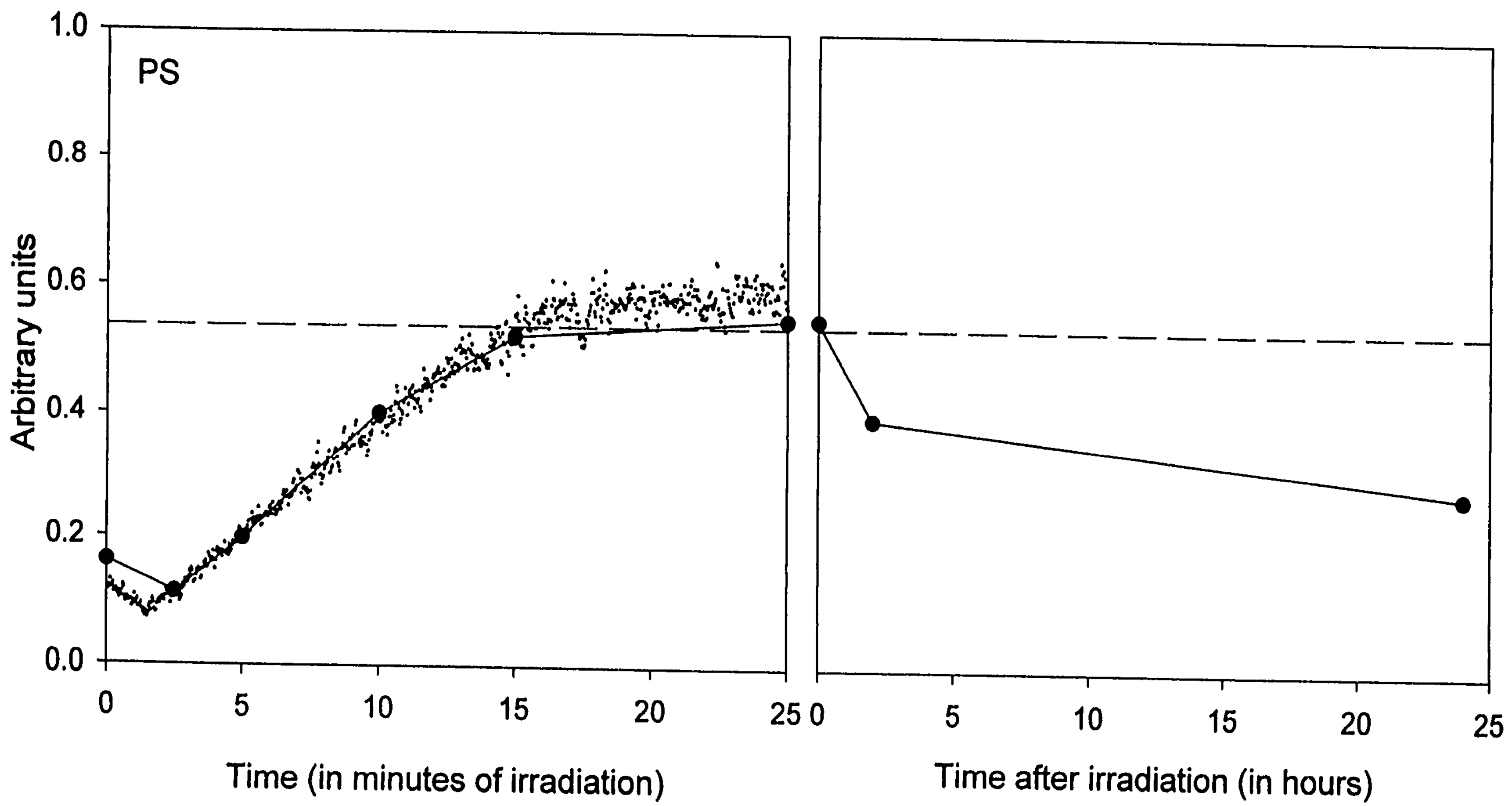

Figure 4.5.5 Evolution of SHG parameters for Si(111)-H surface oxidation over time as a function of UV irradiation in ambient air

4.5.5. Variation of UV irradiance for continuous monitoring

Two different values for the sample to Hg lamp distance were employed for the continuous and incremental monitoring of Si(111)-H oxidation as a function of UV exposure: 10 cm and 15 cm. The irradiance, based on specifications [24], was 0.46 mW/cm^2 and 0.21 mW/cm^2, respectively. From Figure 4.5.6, it is evident that the higher irradiance induced more rapid oxidation, but the final value for γ after 25 minutes in that case or 37.5 minutes of exposure for the lower irradiance, was similar within the variation observed for repeat experiments. There appears to be a saturation level for the oxidation with UV exposure. This plateau seems to correlate with intrabilayer insertion for the topmost bilayer and interbilayer insertion of oxygen, which essentially corresponds to half the thickness of a native oxide sample, which can be thought of as bulk silicon with the two topmost bilayers completely oxidized. With the lamp placed at 15 cm, the drop in γ was a shallow well, suggesting that the intrabilayer insertion is a gradual process, approximately occurring over the first 7.5 minutes. Then, the slope of the increase in γ, when interbilayer insertion polarizes the Si-Si back bonds of the second bilayer, was not very steep. The data for twice the irradiance had a deeper well, which was obtained over the initial 2.5 minutes of UV exposure. The rise in γ was much sharper and, after 19 minutes, it reached a maximum. At the lower irradiance, this point did not happen until the sample was subject to at least 27 minutes of irradiation. This indicates that the increase in oxidation rate is not linear with respect to the increase in irradiance.

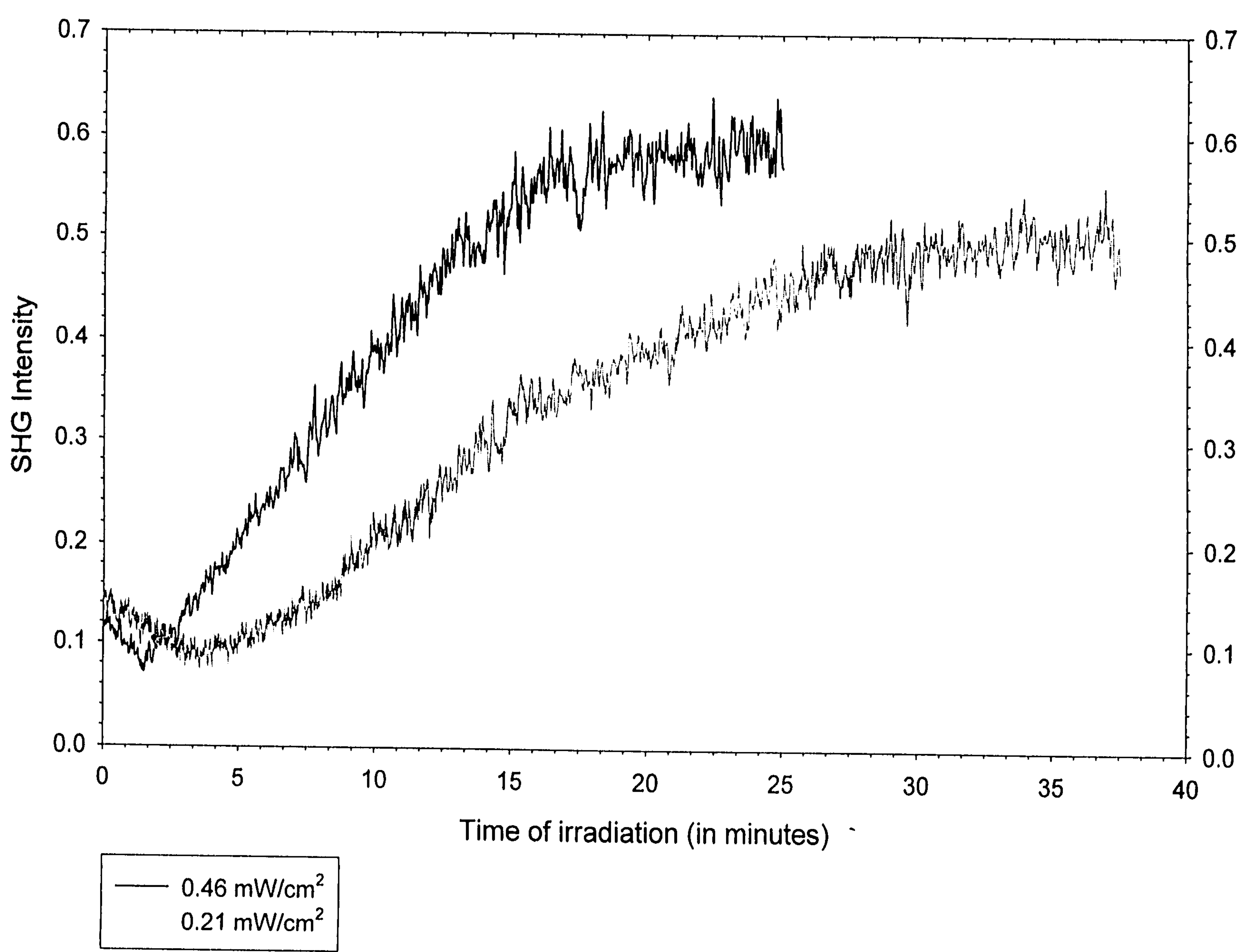

Figure 4.5.6 Continuous monitoring of the anisotropic signal for Si(111)-H surface oxidation over time as a function of UV irradiance

This study, involving only two different irradiance levels, could be extended to include higher irradiance to investigate whether there is a threshold beyond which the oxidation cannot occur any more rapidly. A consideration in this case of high irradiance is sample damage. Likewise, if a lower irradiance level was examined, the process of Si(111)-H oxidation by ambient air would influence the results as the UV light would be relatively weak, possibly making the contributions from each of these competing sources of oxidation difficult to separate. Continuous monitoring is more conclusive than incremental monitoring as the appearance of a plateau in the signal intensity is more readily observable.

4.6. Chemical mechanism for Si(111)-H oxidation

The oxidation of Si(111)-H in ambient air in the dark and the oxidation of Si(111)-H in the presence of UV irradiation appear to manifest the same type of behavior over time, which has been correlated to a layer-by-layer mechanism involving insertion of atomic oxygen into the Si-Si bonds of the substrate. Several possibilities exist with respect to how the attack by water and/or molecular oxygen actually occurs to result in Si-O-Si bridge bonds.

Chidsey et al. [18] propose that photo-oxidation of the Si(111)-H surface proceeds via a radical chain reaction mechanism where the Si-H bond is dissociated by UV illumination. Radiation from a Hg pen lamp at 254 nm (4.89 eV) has more than enough energy to break the Si-H bond (3.5 eV) and create a Si dangling bond. They suggest that dioxygen

adds to this dangling bond to form a Si-O-O$^\bullet$ bond. A neighboring surface hydrogen is abstracted by the newly formed peroxy radical, which initiates a chain reaction to generate additional surface dangling bonds available for reaction with dioxygen molecules, with the eventuality of a completely oxidized surface. It is not well understood how the oxygen then penetrates into the substrate's Si-Si back bonds and the Si-H bonds at the surface are regenerated, but there is FTIR spectral evidence [18] for the occurrence of these phenomena. The free radical mechanism and subsequent back bond insertion is supported by the case of *tris*-trimethylsilylsilane reacting with oxygen, where the addition of a free radical scavenger inhibits the reaction and the first isolated product contains Si-O-Si bridge bonds [25].

Another possible mechanism for the photo-oxidation of Si(111)-H is electron capture from the surface by molecular oxygen to form superoxide anions, O_2^-, which serve to initiate the substrate oxidation.

Attack of Si-Si back bonds by water could occur by the mechanism depicted in Figure 4.5.7. The oxygen of the water molecule has a negative dipole, so it aligns with the positively polarized surface silicon atom. The Si-Si bond is cleaved and, following the evolution of hydrogen gas, the Si-O-Si bridge is formed. It is not known how crucial moisture is for photo-oxidation, but for reaction in ambient air, it plays a large role with respect to the rate and extent of oxidation [13].

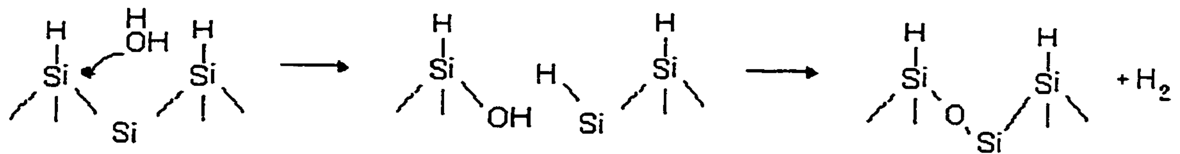

Figure 4.5.7 Water attack of Si-Si back bonds of a Si(111)-H surface

Another possibility, which is suggested by Niwano et al. [13], is the attack of water at the Si-H bond, leading to a penta-coordinated silicon intermediate with rapid evolution of hydrogen gas to leave a hydroxylated silicon surface, as shown in Figure 4.5.8. The manner in which the atomic oxygen then migrates into the back bonds to form Si-O-Si bridge bonds is not known. It is not clear at which point in the oxidation process that the Si-H bonds are eliminated completely from the surface, nor exactly what the surface structure is after extensive exposure in air. Molecular oxygen appears to preferentially insert into the Si-Si back bonds, but the mechanism has not been elucidated. There is scope for numerous experiments to be performed in order to clarify the processes, which govern the surface oxidation of Si(111)-H.

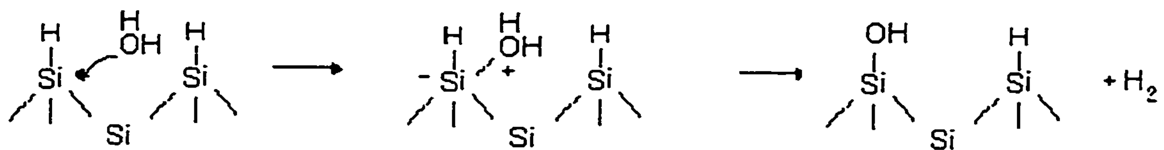

Figure 4.5.8 Water attack of the Si-H bond of a Si(111)-H surface

References

1 Tsang, T. Y. F., Phys. Rev. A **52**, 4116 (1995)

2 Sipe, J. E., Moss, D. J. and van Driel, H. M., Phys. Rev. B **35**, 1129 (1987)

3 Bottomley, D. J., Lüpke, G., Mihaychuk, J. G. and van Driel, H. M., J. Appl. Phys. **74**, 6072 (1993)

4 Mitchell, S. A., Boukherroub, R. and Anderson, S., J. Phys. Chem. B **104**, 7668 (2000)

5 Sieger, M. T., Luh, D. A., Miller, T., Chiang, T. -C., Phys. Rev. Lett. **77**, 2758 (1996)

6 Mitchell, S. A., Boukherroub, R. and Anderson, S., unpublished results.

7 Boukherroub, R., Morin, S., Sharpe, P., Wayner, D. D. M. and Allongue, P., Langmuir (2000) in press

8 Boukherroub, R., Morin, S., Bensebaa, F. and Wayner, D. D. M., Langmuir **15**, 3831 (1999)

9 Ye, S., Ichihara, T. and Uosaki, K., Appl. Phys. Lett. **75**, 1562 (1999)

10 Linford, M. R., Fenter, P., Eisenberger, P. M. and Chidsey, C. E. D., J. Am. Chem. Soc. **117**, 3145 (1995)

11 Mitchell, S. A., Mehendale, M., Villeneuve, D. M. and Boukherroub, R., Chem. Phys. Lett. submitted

12 Higashi, G. S., Chabal, Y. J., Trucks, G. W. and Raghavachari, K., Appl. Phys. Lett. **56**, 656 (1990)

13 Niwano, M., Kageyama, J., Kurita, K., Kinashi, K, Takahashi, I. and Miyamoto

N., J. Appl. Phys. **76**, 2157 (1994)

14 Miura, T., Niwano, M., Shoji, D. and Miyamoto, N., Appl. Surf. Sci. **100/101**, 454 (1996)

15 Morita, M., Ohmi, T., Hasegawa, E., Kawakami, M. and Ohwada, M., J. Appl. Phys. **68**, 1272 (1990)

16 Higashi, G. S., Becker, R. S., Chabal, Y. J. and Becker, A. T., Appl. Phys. Lett. **58**, 1656 (1991)

17 Teraishi, K., Takaba, H., Yamada, A., Endou, A., Gunji, I., Chatterjee, A., Kubo, M., Miyamoto, A., Nakamura, K. and Kitajima, M., J. Chem. Phys. **109**, 1495 (1998)

18 Cicero, R. L., Linford, M. R. and Chidsey, C. E. D., Langmuir **16**, 5688 (2000)

19 Mitchell, S. A., unpublished results

20 Yu, H.-Z. and Mitchell, S. A., unpublished results

21 Raider, S. I., Flitsch, R. and Palmer, M. J., J. Electrochem. Soc. **122**, 413 (1975)

22 Wojtyk, J. T. C. and Wayner, D. D. M., unpublished results

23 Ulman, A., Chem. Rev. **96**, 1533 (1996)

24 Reader, J., Sansonetti, C. J. and Bridges, J. M., Appl. Optics **35**, 78 (1996)

25 Chatgilialoglu, C., Guarini, A., Guerrini, A., Seconi, G., J. Org. Chem. **57**, 2207 (1992)

5. Conclusions

The surface substituent on a Si(111) substrate affects the SHG response by influencing the degree of polarization of the Si-Si back bonds. The electronegativity of the species covalently attached to the surface silicon atoms is correlated with an enhancement of the signal. If a surface is initially terminated by a moderately electronegative substituent and it undergoes a reaction where the substituent is replaced with a significantly more electronegative species, the distinct contrast can be observed with a SHG probe. Because the technique takes advantage of the changes in SHG parameters during the course of chemical transformation, SHG shows promise as a tool for characterizing reactions *in situ*. The formation of a Si(111)-Cl surface in a UV photo-induced reaction in liquid CCl_4 has been studied in this manner [1]. In this work, the oxidation of a Si(111)-H surface was followed both in an incremental and continuous fashion to elucidate the changes in the isotropic, A and anisotropic, B components of the signal. The surface was held in ambient air, either in the dark or with 254-nm UV irradiation to accelerate the reaction.

The Si(111) surface possesses threefold symmetry and exhibits rotational anisotropy. For p-polarized second-harmonic radiation, an isotropic and anisotropic component of the signal can be extracted from the resultant plot when the sample is rotated through 360°. Alternately, the anisotropic component can be isolated by orienting the sample at 30°, as measured between the plane of incidence and a <2-1-1> direction on the wafer, keeping the sample stationary and using the (p,s) polarization configuration to record the signal.

The point of primary interest for the evolution over time of the SHG signal for the oxidation of Si(111)-H is the non-monotonic behavior observed for both UV-irradiated samples and those exposed only to ambient air. The A and B values initially decreased after fresh preparation of the Si(111)-H surface, then an increase was observed, followed by a subsequent decrease, and, over long periods of time, another increase was apparent. These stages of the surface oxidation were interpreted with the aid of a simple model, which suggests that A and B values are proportional to the number of Si-Si bonds present in the substrate. According to this model, when a Si-Si bond is oxidized, it no longer contributes to the SHG signal. Furthermore, supported by precedent in the literature [2,3], a layer-by-layer mechanism for the oxidation was proposed.

In this interpretation, oxidation initially occurs at the surface Si-Si back bonds, termed intrabilayer insertion; subsequently, interbilayer insertion of oxygen takes place and oxidation proceeds deeper into the substrate. Essentially, the relative decrease or increase of the SHG signal is determined by whether, respectively, intra- or interbilayer insertion predominates at any given point during the Si(111)-H oxidation. The mechanism for the attack by oxidizing species is not well understood, though it is suggested that water plays a crucial role in oxidation [4] and molecular oxygen is an ancillary factor. By means of a nitrogen purge environment, it was proven that the limited exposure to moisture and oxygen inhibited any significant oxidation of the Si(111)-H surface.

Although photo-oxidation of the Si(111)-H surface exhibited the same non-monotonic behavior of the SHG signal as for the exposure to ambient air in the dark, it is not clear

whether moisture is an equally important condition in this case or whether molecular oxygen is the prime oxidizing species, inserting into the substrate via a free radical chain reaction mechanism or via electron capture at the surface, which produces superoxide anions.

In contrast to the hydrogen terminated surface, Si(111) surfaces chemically modified with organic monolayers were more robust to oxidation in ambient air. In particular, the decyl terminated surface showed no change in its SHG signal over three weeks of exposure. Decyloxy modified Si(111) can be prepared via two different starting reagents, either decanal or decanol. It has been shown that the latter method yields an organic film with structures that are more hydrolyzable [5], thus its stability in air was considerably lower than for the aldehyde route to decyloxy modification.

The intensity of an SHG response depends on the chemically bonded species at the surface, so it is not subject to the problems encountered in IR studies, arising from any physisorbed organic contaminants on the surface. The inherent sensitivity towards monolayer composition and the ability to monitor samples in air makes SHG a flexible and straightforward way to investigate Si(111) samples with different surface chemical modifications.

References

1 Mitchell, S. A., Boukherroub, R. and Anderson, S., J. Phys. Chem. B **104**, 7668 (2000)

2 Miura, T., Niwano, M., Shoji, D. and Miyamoto, N., Appl. Surf. Sci. **100/101**, 454 (1996)

3 Morita, M., Ohmi, T., Hasegawa, E., Kawakami, M. and Ohwada, M., J. Appl. Phys. **68**, 1272 (1990)

4 Niwano, M., Kageyama, J., Kurita, K., Kinashi, K, Takahashi, I. and Miyamoto N., J. Appl. Phys. **76**, 2157 (1994)

5 Boukherroub, R., Morin, S., Sharpe, P., Wayner, D. D. M. and Allongue, P., Langmuir (2000) in press

6. Future Work

There are several avenues worth pursuing with respect to the oxidation of Si(111)-H surfaces. The photo-oxidation process is of interest because of its potential to produce patterned surfaces by using a mask to selectively irradiate portions of a wafer. This capacity could also be paired with organic monolayer modification and/or bio-functionalization of the surface.

It is of particular interest to investigate the influence of moisture and molecular oxygen on the rate of photo-oxidation and how each contributes to the back bond insertion process. The Si(111)-H surface could be subject to several different environments during oxidation such as dry O_2 or wet N_2 to isolate each oxidizing species. Labeled gases ($H_2{}^{18}O$ or $^{16}O_2$) could help determine the fate of the Si-H surface bonds via secondary ion mass spectrometry (SIMS) measurements. To round out these experiments, studies in air with different percentages of relative humidity would incorporate the influence of both oxidizing species.

The variation of irradiance for the photo-oxidation of Si(111)-H was not studied in detail. Further investigation of several different intensities and lengths of time for the UV irradiation would provide information about the rate of oxidation and its efficiency. This could possibly allow custom design of the extent of oxide formation desired on a surface.

There would be merit in using other surface characterization techniques to support the results determined using SHG. Ellipsometry, XPS and FTIR spectroscopies would all complement the present work on Si(111)-H and oxidation in ambient air and by UV irradiation. It would be most useful if the same sample was subject to a number of techniques in sequence. In this way, the stages of oxidation could be well defined by combining the strengths of each method, thus obtaining measurements of several parameters for a given Si(111)-H surface. Other reactions could be the subject of SHG experiments; this would build a library of rotational anisotropy plots identifying particular terminating species. These data would be useful for determining the success of sequential organic modifications or changes caused by UV irradiation.

Undertaking experiments, at wavelengths which correspond to resonance enhancement, would make the differences between the native oxide SHG signal and the chemically modified Si(111) surfaces more dramatic. SHG at silicon surfaces is resonantly enhanced when the second-harmonic photon is close to a direct-gap excitation of bulk silicon [1]. The lowest energy direct-gap excitations lie in the region of 365 nm. Maximizing the sensitivity of the probe wavelength improves the capability of SHG to act as an optical method for monitoring chemical reactions at silicon surfaces *in situ*.

The potential of SHG is only beginning to be recognized as optimum laser sources, namely short pulse and high intensity, have only been commercially available for less than a decade. Similarly, with the introduction of a method for ideal termination of the Si(111)-H surface [2] occurring not long ago either, researchers have not exploited the

capacity for this substrate to revolutionize microelectronic and semiconductor devices beyond the tip of the proverbial iceberg.

References

1 Mitchell, S. A., Mehendale, M., Villeneuve, D. M. and Boukherroub, R., Chem. Phys. Lett. submitted

2 Higashi, G. S., Chabal, Y. J., Trucks, G. W. and Raghavachari, K., Appl. Phys. Lett. **56**, 656 (1990)